NASA Technical Memorandum ~~102182~~

An Experimental Investigation of Helicopter Rotor Hub Fairing Drag Characteristics

D. Y. Sung, M. B. Lance, L. A. Young,
and R. H. Stroub

September 1989

National Aeronautics and
Space Administration

NASA Technical Memorandum 102182

An Experimental Investigation of Helicopter Rotor Hub Fairing Drag Characteristics

D. Y. Sung, Sterling Software Corporation, Palo Alto, California
M. B. Lance, Planning Research Corporation, Hampton, Virginia
L. A.Young and R. H. Stroub, Ames Research Center, Moffett Field, California

September 1989

NASA

National Aeronautics and
Space Administration

Ames Research Center
Moffett Field, California 94035

CONTENTS

SYMBOLS

A_{ref}	reference area = frontal area of the fuselage, 1.43 ft^2
C_D	drag coefficient, $D/(q\ A_{ref})$
CD_I	total mutual interference drag between fuselage, pylon, and hub fairing
CD_t	total drag of fuselage+pylon+hub fairing
CD_f	isolated fuselage drag
$CD_{f/h}$	fuselage-on-hub interference drag
CD_{fh}	mutual interference drag of the fuselage+hub fairing
CD_{fp}	mutual interference drag of the fuselage+pylon
$CD_{f/p}$	fuselage-on-pylon interference drag
CD_h	isolated hub fairing drag
$CD_{h/f}$	hub-on-fuselage interference drag
$CD_{h/p}$	hub-on-pylon interference drag
CD_p	isolated pylon drag
$CD_{p/f}$	pylon-on-fuselage interference drag
CD_{ph}	mutual interference drag of the pylon+hub fairing
$CD_{p/h}$	pylon-on-hub interference drag
C_L	lift coefficient, $L/(q\ A_{ref})$
C_{PM}	pitch moment coefficient, $PM/(q\ L_{ref}\ A_{ref})$
C_{RM}	roll moment coefficient, $RM/(q\ L_{ref}\ A_{ref})$
C_{SF}	side force coefficient, $SF/(q\ A_{ref})$
C_{YM}	yaw moment coefficient, $RM/(q\ L_{ref}\ A_{ref})$
D	drag, lb
DQ	equivalent flat plate drag area, D/q (ft^2)
g	hub/pylon fairing gap width, ft
h	hub fairing height, bottom of fairing to top of fuselage, ft
L	lift, lb
L_{ref}	reference length, 1.26 ft
LQ	lift to dynamic pressure ratio, L/q (ft^2)
PM	pitch moment, ft-lb
q	dynamic pressure = $1/2\ r\ V_\infty^2$ (psf)
RM	roll moment, ft-lb
SF	side force, lb

V_∞ free-stream velocity, ft/sec

YM yaw moment, ft-lb

a angle of attack, deg

d_{axial} uncertainty in an axial load measurement of the strain gage balance, lb

d_{normal} uncertainty in a normal load measurement of the strain gage balance, lb

d_{pitch} uncertainty in a pitch moment measurement of the strain gage balance, in-lb

d_{roll} uncertainty in a roll moment measurement of the strain gage balance, in-lb

d_{side} uncertainty in a side force measurement of the strain gage balance, lb

d_{yaw} uncertainty in a yaw moment measurement of the strain gage balance, in-lb

r density, slug/ft ^{3}

SUMMARY

A study was done in the NASA 14- by 22-Foot Wind Tunnel at Langley Research Center on the parasite drag of different helicopter rotor hub fairings and pylons. Parametric studies of hub-fairing camber and diameter were conducted. The effect of hub fairing/pylon clearance on hub fairing/pylon mutual interference drag was examined in detail. Force and moment data are presented in tabular and graphical forms. The results indicate that hub fairings with a circular-arc upper surface and a flat lower surface yield maximum hub drag reduction; and clearance between the hub fairing and pylon induces high mutual-interference drag and diminishes the drag-reduction benefit obtained using a hub fairing with a flat lower surface. Test data show that symmetrical hub fairings with circular-arc surfaces generate 77% more interference drag than do cambered hub fairings with flat lower surfaces, at moderate negative angle of attack.

1. INTRODUCTION

Rotor hub and pylon drag constitute 20-30% of the total parasite drag of single rotor helicopters (refs. 1-3). Since parasite drag represents 40-50% of the total power requirement of a single rotor helicopter (ref. 3), the drag of the rotor hub represents roughly 10% of the total power required. The fuel savings from the reduction of helicopter rotor hub drag has stimulated many research efforts. Furthermore, current civilian and military requirements call for helicopters with high speed and long range capabilities, and therefore low drag is an important design criterion.

The idea of using a hub fairing to streamline the rotor hub dates from the late nineteen-fifties. One of the earliest studies of isolated hub fairing drag with different fairing thickness and camber was done by Sikorsky Aircraft (ref. 4). Bell Helicopter Company and the Boeing Company Vertol Division also have conducted some studies of rotor hub fairings (refs. 5-7).

Besides the work of developing low-drag hub fairing and pylon components, researchers are faced with a major obstacle when solving the hub-drag problem: the additional drag engendered by the aerodynamic interactions between the hub fairing and pylon. Because this interference drag could amount to 35% of the total hub and pylon drag (ref. 3), it remains a major barricade to the successful development of low-drag hub fairings. A research program was initiated at NASA Ames Research Center to study the aerodynamic interactions and interference drag between hub fairing and pylon. The goal of the Ames Hub Drag Reduction Research Program is to devise hub fairing designs that can achieve 50-80% hub/pylon drag reduction.

As part of this program, two small-scale wind tunnel tests were conducted in the NASA Ames 7- by 10-Foot Wind Tunnel to investigate the drag characteristics of new hub fairing and pylon design concepts (refs. 8-12). A substantial data base was established on the effects of various hub fairing and pylon aerodynamic attributes on hub drag reduction. However, since additional information was needed to further this hub drag reduction effort, a third wind tunnel test was conducted in the NASA Langley 14- by 22-Foot Wind Tunnel. The data from this test are presented in this paper.

The main objectives of the Langley 14- by 22-Foot Wind Tunnel test were to (1) confirm the test methodology used in the earlier Ames 7- by 10-Foot Wind Tunnel hub drag tests by correlating data from independent test setups; (2) identify aerodynamic characteristics of different hub and pylon fairing designs; and (3) conduct a more extensive study of the effect of hub/pylon clearance on hub/pylon interference drag.

The wind tunnel test used a 1/5-scale model of the XH-59A as the baseline fuselage upon which various hub and pylon fairing assemblies were mounted. The hub assemblies were nonrotating. Data acquired were drag, lift, side force, yawing moment, rolling moment, and pitching moment. This report presents major findings of the test. Included are all the aerodynamic load data in tabulated form, and the graphical presentation of the drag data. Test configurations and data reliability are discussed.

2. TEST APPARATUS AND DATA ACQUISITION, RELIABILITY, AND PRESENTATION

2.1 Test Apparatus

The 1/5-scale XH-59A model was used as the baseline fuselage. The XH-59A is the Advancing Blade Concept Helicopter developed by the Sikorsky Aircraft Division of United Technologies Corporation. The XH-59A model had been tested extensively in the Ames 12-Foot Pressure Wind Tunnel and the 7- by 10-Foot Wind Tunnel with both nonrotating (refs. 8,9) and rotating (ref. 13) hardware. Instead of the dual-hub configuration used in the Advancing Blade Concept, a single-hub configuration was used in this test.

The model installation is shown in figure 1. The hub and shaft fairings were mounted on a nonrotating shaft. The model was sting-mounted, and used an internal strain-gage balance as the load-measurement unit. The mounting scheme as well as the dimensions of the model are given in figure 2.

2.2 Data Acquisition and Reduction

Quantitative data in the form of six component forces and moments were obtained by an internal strain-gage balance. Each data point taken was an average of 40 sample points. All data reduction was done using a MODCOMP Classic computer where weight tare corrections and the balance-axis-to-wind-axis transformation were applied to the raw data.

Data were acquired for a range of dynamic pressures and model pitch angles at zero yaw angle. Dynamic pressure sweeps were conducted at 0° angle of attack, with dynamic pressure varying from 40 psf to 120 psf in increments of 20 psf. Most of the runs were pitch angle sweeps tested at a dynamic pressure of 80 psf with the angle of attack varying from -10° to 2° in increments of 2°. The reference coordinate system used in data reduction is shown in figure 3.

The force and moment data are presented in coefficient form. The frontal area of the fuselage, $A_{ref} = 1.43$ ft^2, was used as the reference area to normalize the force data. The height of the fuselage cross section, 1.26 ft, was used as the reference length, L_{ref}.

2.3 Tunnel Corrections

Corrections of solid blockage and wake blockage effects were deemed unnecessary because the model blockage was less than 1% of the test section area. The model was unpowered and the span of the only lifting surface, the hub fairing, was less than 14% of the tunnel span; therefore, wall interference effects and jet boundary corrections were not applied to the data. Other effects, such as tunnel buoyancy, were also negligible. The internal mounting scheme obviated the correction for sting tares, and no attempt was made to account for the sting-on-fuselage interference drag.

2.4 Accuracy of the Internal Strain-Gage Balance

The accuracies of the force and moment measurements from the internal balance were within 0.5% of the corresponding maximum load of each measurement component. The resolution of the balance in engineering units is given below:

$$\delta_{axial} = \pm 0.375 \text{ lb}$$

$$\delta_{normal} = \pm 8.000 \text{ lb}$$

$$\delta_{side} = \pm 2.500 \text{ lb}$$

$$\delta_{pitch} = \pm 1.25 \text{ ft-lb}$$

$$\delta_{roll} = \pm 0.625 \text{ ft-lb}$$

$$\delta_{yaw} = \pm 0.625 \text{ ft-lb}$$

The drag, lift, side force, pitch moment, roll moment, and yaw moment of the aerodynamic loads were measured by the axial, normal, side, pitch, roll, and yaw gages of the balance, respectively. At a dynamic pressure of 80 psf, the drag level of the low-drag test configuration (H50,S40) was about 14 lb; therefore, at most a 3% uncertainty in measured drag could be ascribed to inaccuracy of the balance.

2.5 Data Repeatability

In order to study the repeatability of the test data, the H50,S40 configuration (see section 3.1) was tested on two different days with many configuration changes. Figure 4 displays the drag data (in engineering units) of the two repeated runs. The repeated data fell within an acceptable range of uncertainty dictated by the resolution of the internal balance.

2.6 Reynolds Number Effects

Reynolds number effect or scale effect on the drag measurement of the H50,S40 test configuration (see section 3 for definitions of test configurations) is shown in figure 5. Problems relating to the Reynolds number effects on the drag measurements of helicopter models (high-drag bodies) have been well noted in the past (refs. 14,16). However, the test data reported here exhibit only a very slight dependence on the Reynolds number based on the height of the fuselage; that is, within the range of

tested Reynolds numbers, no noticeable transitional effect has been observed. Most of the data presented were taken at a Reynolds number of 1.5×10^6/ft.

3. TEST CONFIGURATIONS AND TEST SWEEPS

3.1 Test Configurations

All test configurations were given a two-digit designation for easy reference. The test matrix given in table I shows how the test was structured, and it can be used as a quick reference to the test configurations. Test configurations were defined based on a combination of geometric parameters, shown in figure 6.

1. Hub fairings. Basically, a hub fairing is designed to reduce the aerodynamic drag of the rotor hub in forward flight. All of the hub fairings tested have a circular planform. The profiles of the hub fairing cross sections are of key interest. Hub fairing profiles with different camber, diameter, and thickness ratio were studied, and were identified with a two- or three-digit designation with an H prefix. The following hub fairings were tested: H10, H20, H30, H40, H50, H60, H220, H230, H240, H250, H260, H270, and H280. See figures 7-10 for the profiles of these hub fairings.

2. Pylons (shaft fairings). The use of a pylon, or shaft fairing, is similar to that of the hub fairing except that the pylon is used to fair the rotor shaft. Pylons were identified with a two-digit designation with an S prefix. Two configurations were tested: S40 and S80. The cross sections of these shaft fairings are shown in figure 11.

3. Hub/pylon gap width. The gap (or clearance) between the hub fairing and the pylon has been observed to hamper the effectiveness of the hub fairing as a drag-reduction device (refs. 8,9). Therefore, the effect of hub/pylon gap on drag was studied closely in this test. Except as noted, the hub/pylon gap is zero for all configurations.

4. Pylon height. Pylon height is one of the parameters that influences the overall hub/pylon drag, and it is defined as the length of the rotor shaft between the top of the fuselage and the bottom of the hub fairing (fig. 6). Pylon heights of 0.1667 ft, 0.3333 ft, 0.5 ft, and 0.5833 ft were tested with the H50,S40 configuration. All other configurations were tested with a 0.5833-ft pylon height.

5. Wake shield. A wake shield is a streamlined surface placed on the top of the pylon, and it is designed mainly to minimize the interference drag incurred from hub fairing/pylon clearance. It is also referred to in this report as a pylon end plate. A more detailed discussion on the wake shield is presented in the next section. Two different wake shields, designated W1 and W2, were tested.

3.2 Test Sweeps

The test was organized into six test sweeps. This section outlines the purpose of each test sweep and which parameters were varied.

1. Hub fairing camber with constant hub fairing diameter and thickness. This set of hub fairings (H20, H30, H40, H50, and H60) was used to investigate the effect of hub fairing camber on the hub/pylon mutual interference drag (fig. 8). Since the main objective of this test sweep was to study the hub/pylon mutual interference drag, the set of hub fairings was designed to have comparable levels of skin-friction drag and profile drag. This was accomplished by using hub fairings with the same amount of wetted surface area, thickness ratio, and thickness distribution.

2. Hub fairing thickness ratio with constant hub fairing diameter. This set of hub fairings (H50, H220, and H230) was used to investigate the profile drag of hub fairings with a circular-arc upper surface and flat lower surface cross section (fig. 9). The purpose of this sweep was to determine the effects of hub fairing thickness ratio on drag by varying the frontal area of the fairing while keeping the diameter constant. A hub fairing with a higher thickness ratio entails less weight penalty because of a more efficient use of fairing volume. Because the weight of each hub fairing is an important factor in evaluating the attractiveness of a particular design, it is essential to measure the overall effects of hub fairing thickness on drag.

3. Hub fairing thickness ratio with constant hub fairing thickness. This test sweep was devised to study the trade-off between profile drag and skin-friction drag with respect to the change in the hub fairing thickness ratio. This change in thickness ratio (hub fairing H50, H240, H250, H260, H270 and H280; see fig. 10) was done by increasing the fairing diameter while keeping the thickness constant. The cross sections of these fairings have the same geometric attributes: circular-arc upper surface and flat lower surface. The reason for keeping the hub fairing thickness constant is that all the fairings will house the same rotor hub. The circular-arc upper surface and flat lower surface fairing cross section was chosen because it had been shown to be a low-drag configuration in previous wind tunnel tests (refs. 8,9).

4. Pylon height. The scope of this sweep was to measure the pylon+hub fairing drag as a function of pylon height. The potential flow interaction between the hub and fuselage depends directly on the height of the shaft fairing. It is thus desirable to determine the drag trend with respect to the pylon height. In this sweep, the pylon height was varied from 0.1667 ft to 0.5833 ft. The H50,S40 configuration was used.

5. Hub/pylon gap width. In this sweep, attention was focused on the small gap between the hub and pylon. Previous wind tunnel tests indicated that the hub/pylon gap induces a high shaft-on-pylon interference drag. The objective of this test sweep was to measure how this extra drag penalty impacts the drag reduction when using a hub fairing. Both high-drag and low-drag hub fairing designs, H10 and H50, respectively, were selected for this study (fig. 7).

6. Wake shield (or pylon end plate) concept. The purpose of this sweep was to study the potential drag reduction from using wake shields. See figure 12 for drawings of the wake shields tested. The wake shield is attached to the top of the pylon such that the sharp edge of the shield aligns to the free stream.

The clearance between the hub fairing and pylon had been observed to cause high interference drag. The wake shield is a design concept which attempts to minimize the impact of the gap on drag. If the hub/pylon gap cannot be eliminated, the exposed part of the rotor shaft between the hub fairing and the

pylon produces a turbulent wake. At a negative fuselage pitch angle, we may postulate that this turbulent wake, with wake entrainment, may convect downstream and intermix with the boundary layer of the flow over the aft portion of the pylon. Such interaction may disturb the pressure distribution of the flow over the pylon and cause flow separation. In order to avoid the flow separation induced by the wake, and hence the resultant drag penalty, the wake shield, a wide edge plate, is installed atop of the pylon to delay or prevent the turbulent wake from interacting with the flow over the pylon.

4. RESULTS AND DISCUSSION

The data are organized by run number. A cross reference between run number and configuration definitions is provided in tables II and III. The force and moment data are tabulated in the appendix.

Much of the hub-drag data presented here was obtained in order to confirm the methodology used in previous hub drag tests, and therefore most of the configurations had been tested before (refs. 8-12). However, this study went further than previous studies in the following areas:

1. The hub/pylon gap effect on the interference drag was examined more closely in the area in which a large change in drag had been observed previously.

2. The effect of pylon height on drag was studied in detail.

3. More elaborate wake shield designs were tested.

For completeness, discussions of all of the test results are included in the following sections. Some of the observations reiterate important findings published previously; the reader should refer to references 8-12 for the original work on hub fairing development.

4.1 Data Correlation with the Ames 7- by 10-Foot Wind Tunnel Test Data

This section presents correlations between the Langley 14- by 22-Foot Wind Tunnel test data and the Ames 7- by 10-Foot Wind Tunnel test data (ref. 11). Care was taken to ensure proper matching of the model hardware, installation, and experimental configurations between these tests.

Apart from being conducted at different wind tunnel facilities, the two tests differed in one major respect: the 14- by 22-Foot Wind Tunnel test used an internal strain-gage balance, whereas the 7- by 10-Foot Wind Tunnel test used the wind tunnel external scales. By correlating the test data, one can determine whether the following factors introduced unacceptable distortion into the 7- by 10-Foot Wind Tunnel test data:

1. Sting tare correction. In the 7- by 10-Foot Wind Tunnel test, the sting tare amounted to approximately 68% of the total drag measured for most of the test configurations. In addition, the model-on-sting interference effects were not accounted for in the sting tare correction.

2. Wind tunnel blockage effects. Model blockage correction was assumed to be negligible in the 7- by 10-Foot Wind Tunnel test. The model blockage was 3.5% in the 7- by 10-Foot Wind Tunnel test. It was reduced to 0.8% in the 14- by 22-Foot Wind Tunnel test.

Data correlation of four important test sweeps in the 14- by 22-Foot Wind Tunnel test and the 7- by 10-Foot Wind Tunnel test are presented in figures 13-16. From these comparisons, it can be concluded that the model-on-sting interference and the model blockage had only minor impacts on the drag data obtained in the previous 7- by 10-Foot Wind Tunnel tests.

4.2 Interference Effects Between Hub Fairing and Pylon

Data from different wind tunnel tests (ref. 3) clearly indicate that interference drag has encumbered the development of low-drag hub fairings. Mutual interference drag is engendered from the aerodynamic interactions between solid bodies when they are placed in proximity in the free stream. These aerodynamic interactions are potential flow interaction, vortex interaction, and three-dimensional boundary-layer interaction. Because of the interdependent nature of these interactions, a detailed and accurate account of interference drag is impractical to obtain experimentally. It is important, however, that the interference drag be conceptually understood. To aid in our analytical study of the drag data, the following notations will be used in the discussion.

In general,

CD_X = X-body component or isolated drag

$CD_{X/y}$ = X-body-on-Y-body interference drag

$CD_{y/x}$ = Y-body-on-X-body interference drag

CD_{xy} = mutual interference drag between X body+Y body

$= CD_{x/y} + CD_{y/x}$

and specifically,

$$CD_I = CD_{fp} + CD_{ph} + CD_{fh}$$
$$= CD_{f/p} + CD_{p/f} + CD_{p/h} + CD_{h/p} + CD_{f/h} + CD_{h/f}$$
$$= CD_t - CD_f - CD_p - CD_h$$

where

CD_I = total mutual interference drag between fuselage, pylon, and hub fairing.

Three types of drag data were measured: CD_f, $CD_f + CD_p + CD_{fp}$, and CD_t.[1] Without the drag data of each isolated component, it is not possible to quantify the individual interference-drag components. However, with careful reasoning, valuable insight can be obtained from these data.

Interference drag can be examined for a case in which the interference effects were readily apparent. In figure 17, the drag as a function of the pitch angle is displayed for the following configurations: fuselage alone, fuselage + S40 pylon, and fuselage + S40 pylon + H50 hub fairing. From this plot we can observe the drag buildup from adding the pylon and then the hub fairing to the fuselage; that is, we are looking at the magnitudes of CD_f, $CD_f + CD_p + CD_{fp}$ and $CD_f + CD_p + CD_h + CD_{fp} + CD_{ph} + CD_{fh}$. It may be noticed immediately that $CD_{ph} + CD_h + CD_{fh}$ assumed a negative value at negative pitch angles. In other words, the drag reduction caused by the aerodynamic interactions between the H50 fairing and S80 pylon exceeded the additional component drag of the hub fairing. We should also note that the negative magnitude of $CD_{ph} + CD_h + CD_{fh}$ diminished as the angle of attack increased, and $CD_{ph} + CD_h$ became positive at $\alpha = 0^\circ$.

An explanation of the negative CD_{ph} is given as follows. In the case of the fuselage + S40 pylon configuration, when the pylon is set at a negative pitch angle, the flow over the top surface of the pylon, under a favorable (negative) pressure gradient, tends go around the corner to the side surfaces of the pylon in an effort to align with the free stream. At the right-angle corner of the S40 pylon, a local flow separation, a separation bubble, is formed because of the failure of the flow to negotiate the abrupt change in pressure gradient at the corner. Figure 18 is a depiction of this scenario. However, with the H50 hub fairing placed atop the pylon, covering most of its upper surface, the flow is redirected over the upper surface of the fairing, and the area of separation created at the corner of the pylon is thus prevented. Based on the above reasoning, it can further be asserted that the drag reduction caused by the elimination of local flow separation at the side surfaces of the pylon is higher than the skin friction and profile drag of the H50 hub fairing.

At a positive angle of attack and in the absence of the hub fairing, a local flow separation is likely to occur on the top surface of the pylon. However, the area of the top surface tangential to the free stream is much less than that of the side surfaces at small incidence angles. Consequently the drag penalty caused by the corner flow separation is small, at $\alpha = 0\text{-}2^\circ$. On the other side, the induced drag of the cambered hub fairing, a lifting surface, becomes a contributing entity at a positive incident angle. Therefore, the negative CD_{ph} decreases and CD_h increases as the pitch angle becomes more positive. It follows that the drag reduction caused by the favorable interaction between the hub fairing and pylon diminishes at positive angles of attack.

The data thus demonstrate that the aerodynamic interactions between the hub fairing and pylon have a major impact on the effectiveness of different hub fairing designs.

---

[1] Because of the simultaneous interactions between all of the aerodynamic bodies placed in proximity, the interference drag between any two of the components is influenced by the presence of the other components. Likewise, the mutual interference drag between the pylon and fuselage, CD_{fp}, is influenced by the presence of the hub fairing. In this report, it is assumed that the change in CD_{fp} due to the presence of the hub fairing is negligible. CD_{fp} is treated as a constant in the discussion.

4.3 Hub Fairing Camber and Surface Curvature

Previous tests indicated that a hub fairing with positive camber can yield substantial hub drag reduction in forward flight (refs. 8,12). The present effort was a parametric study of the effect of hub fairing camber on drag. The hub fairings were designed to have the same diameter, thickness ratio, and thickness distribution (fig. 8). The wetted surface areas of these hub fairing are also very similar. Therefore, the skin-friction drag and the profile drag of this series of fairings are comparable.

Figure 19 displays the drag as a function of the hub fairing camber. The data suggest that a hub fairing with a 9% camber yields minimum drag. There was a precipitous drop in drag when the camber was at 9% with both the S40 and the S80 pylons. Subtracting the fuselage drag, the 9%-cambered H50 fairing shows a drag reduction, when compared with the 0%-cambered H20 fairing, of 85% with the S80 pylon and 74% with the S40 pylon. If one ascribes the substantial drag reduction to the camber of the hub fairing, then one is obliged to find out how the camber causes such drag reduction, and why the drag reaches a minimum at the particular camber of 9%. After a careful review of the data, an alternative cause-effect relation can be seen.

First, let us focus our attention on the lower aft surface of the hub fairing. Because the rotor shaft is cylindrical in cross section, it is likely that flow separation occurs on the lower aft surface of the hub fairing just behind the shaft. Because the local flow separation has a stronger adverse pressure gradient (caused by positive surface gradient), it is more extensive on the H20, H30, and H40 fairings than on the H50 fairing. Moreover, for those hub fairings with positive lower surface curvature, the flow over the lower surface will be restricted even more when the hub fairing is placed tightly on the top surface of the pylon. Such a flow condition escalates flow separation and produces higher pressure drag. Therefore, hub fairings with a positive lower surface curvature, with more area tangential to the free stream, have higher pylon-on-hub-fairing interference drag, $CD_{p/h}$, than fairings with flat lower surfaces have.

Secondly, hub fairings with a flat lower surface have favorable interactions with the pylon (see section 4.1). In contrast, for the H20, H30, and H40 fairings, the corner flow separation is aggravated by the accelerating flow at the leading edge of the fairing because of the positive lower surface curvature. Concomitantly, the reductions in both $CD_{h/p}$ and $CD_{p/h}$ reduce the drag of the H50 fairing to a much lower level than that of the H20-40 series fairings.

The above reasoning offers a plausible explanation for the substantial drag reduction achieved by using the H50 hub fairing. The drag reduction can be ascribed to the effect of the lower surface curvature. It is reasonable to dismiss the 9% camber as the primary cause of the drag reduction.

We now turn our attention to why the drag-reduction benefit was more pronounced when the S80 pylon was used. If we consider the flow over the S80 profile, we can see that there is a strong adverse pressure gradient (a consequence of high surface gradient) on the pressure-recovery region between 0.2 chord length and 0.7 chord length. That is, the boundary layer formed over the S80 pylon is less stable than that over the S40 pylon, which has a more moderate surface gradient distribution. The boundary layer on the S80 pylon is more prone to flow separation and thus is more sensitive to interference effects. It follows that even small interference effects between the hub fairing and pylon may trigger flow separation of the unstable boundary layer over the S80 pylon. However, when interactions with

the pylon are favorable, as when fairings with a flat lower surface are used, the boundary layer of the S80 pylon remains attached, and substantial drag reduction is observed.

4.4 Hub Fairing Thickness Ratio

Hub fairings with circular-arc upper surfaces and flat lower surfaces were used to study the trade-off between profile drag and skin-friction drag with respect to the change in the hub fairing thickness ratio. Figure 20 shows the drag trend with respect to the hub fairing thickness ratio at two different pitch angles. In this case the change in hub fairing thickness ratio was accomplished by increasing the fairing diameter while keeping the fairing thickness constant. Note that the H280 fairing, with more wetted surface, represents high skin-friction drag; while the H240 fairing, with a larger thickness ratio, represents high profile drag.

At moderate angles of attack, from 3° to -3°, the data indicate that profile drag and skin friction drag were nearly even. The overall drag reached a minimum at a thickness ratio of 20%. At a more negative angle of attack, about -6°, the profile drag caused a higher penalty than did the skin-friction drag. That is, the drag increase was substantial with a thickness ratio of 25% or more. It may also be concluded that a hub fairing with a 20% thickness ratio is less sensitive to change in pitch angle, and yields minimum drag.

An additional study examined the profile drags of the same type of hub fairings with the same diameter but different thicknesses (see fig. 9). The data, plotted in figure 21, clearly indicate that the drag increased with the thickness ratio within the range studied.

4.5 Pylon Height

The presence of the pylon and the fuselage can alter both the magnitude and direction of the local velocity in the hub region. Consequently, part of the interference drag can be attributed to the potential flow interaction between the fuselage and the hub fairing. One of the important parameters influencing the potential flow interaction is pylon height. This test sweep was done to determine the pylon+hub fairing drag as a function of pylon height.

Before the data are examined, two important principles of potential flow theory should be noted. First, there is a local increase in dynamic pressure on the top surface of the fuselage. Second, the direction of the flow near a surface tends to align with that surface. It is also clear that if the potential flow interactions between the fuselage and the pylon/hub fairing were negligible, then the drag increase with respect to pylon height would be linear. Figure 22 shows the drag versus pylon height for the H50,S40 configuration at two different angles of attack. The data show a nonlinear trend in drag with respect to the pylon height. This nonlinearity in drag gives credence to the assertion that hub fairing/pylon/ fuselage potential flow interactions had an appreciable influence on the interference drag.

Moreover, the data indicate that there was a favorable effect when the hub fairing was placed close to the fuselage. There are two counteractive factors involved, namely the increase in local velocity and the decrease in angle of attack. The dynamic pressure near the surface of the fuselage is higher than that of the free stream. This causes a higher hub fairing component drag. However, because the flow close to the fuselage tends to align with the surface, the hub fairing component drag is lower because of

the reduction in angle of attack. In this case, the data suggest that the effect of reduction in angle of attack had a greater impact on the drag than did the increase in local dynamic pressure.

A more direct approach to the study of the hub fairing/pylon/fuselage potential flow interactions is to use potential flow codes to calculate the flow field around the fuselage. With potential flow calculation, the changes in magnitude and direction of the local velocity near the fuselage can be accounted for quantitatively. It should also be noted that the interference drag caused by potential flow interactions depends strongly on the actual hub fairing/pylon/fuselage configuration.

4.6 Hub Fairing/Pylon Gap

The detrimental effects of the hub fairing/pylon gap on the drag reduction achieved by using the low-drag hub fairing (H50) were observed in previous wind tunnel tests. In this study, the gap effects were examined more closely, with special attention to a small fairing/pylon gap in which a steep ascent in drag was observed (ref. 11).

Figure 23 shows the drag as a function of the hub fairing/pylon gap for the H50-S40 and H10-S40 configurations. Note that the pylon height was kept constant. In the case of the low-drag hub fairing (H50), the data show that the drag rise was precipitous when the first 0.5-in. of hub fairing/pylon gap was introduced. For the symmetrical hub fairing (H10), the drag was virtually unchanged with a gap of less than 0.08 ft.

For a given shaft length, the shaft produces substantially higher drag than the pylon. Therefore, the drag increase caused by the increase in the exposed shaft in the gap was anticipated. If the interference effects are only a minor factor, the data should have reflected a more linear drag trend.

The following reasoning is offered to account for the nonlinearity of the drag trend. The exposed shaft in the gap creates a turbulent wake, which in turn induces extensive boundary-layer separation in the flow over both the lower aft portion of the hub fairing and the upper aft portion of the pylon. The resulting drag penalty contributes much to the sharp rise in CD_{ph}. Moreover, in the presence of a gap, the flat-lower-surface hub fairing was no longer able to eliminate the corner flow separation (refer to section 4.1), and this further diminished the favorable interactions between the H50 fairing and pylon.

The drag penalty of the hub/pylon gap on the H10 configuration was less significant because the hub/pylon interference drag was already high. The drag actually dropped slightly when the first 0.25-in. of gap was introduced. The reason for this is that the flow on the lower surface of the H10 fairing was less restricted when a small gap was present. That is, the gap allowed the flow more room to turn around the shaft and thus alleviated some of the flow separation at the low aft surface of the H10 fairing. As the gap increased, the high-pressure drag produced by the rotor shaft became dominant.

4.7 Pylon Wake Shields

The reasoning behind the wake shield design concept is summarized in section 3.2. Two wake shield designs (fig. 12) were studied with different pylon/hub fairing configurations. The impacts on drag of the application of these wake shields can be seen in figures 24 and 25. The data indicate that this design concept failed to meet its objectives. Instead of drag reduction, appreciable drag penalty was

observed. This means either that the wake produced by the shaft had only minor impact on the flow over the pylon, or that the extra profile drag of the wake shield exceeded any drag savings.

5. CONCLUDING REMARKS

The principal test results are summarized below:

1. The Langley 14- by 22-Foot Wind Tunnel test results agree with those of the previous Ames 7- by 10-Foot Wind Tunnel hub drag tests. Good correlation between the different test data was observed, substantiating the test methodology in both test programs.

2. Aerodynamic interactions between the fairing and pylon are the fundamental factors that determine the drag level of seemingly similar hub fairing designs. The hub/pylon mutual interference drag contributes significantly to the overall drag reduction. Therefore, hub fairing design should be coupled with the pylon design in order to achieve optimal results.

3. Hub fairings with a circular-arc upper surface and a flat lower surface yield maximum hub drag reduction.

4. The symmetrical hub fairing with circular-arc surfaces (H20) generates 74% more interference drag than the cambered hub fairing with flat lower surface (H50) at moderate angles of attack, 2° to -4°.

5. A gap between the hub fairing and pylon induces high mutual interference drag and diminishes the drag-reduction benefit obtained by using a hub fairing with a flat lower surface.

APPENDIX: TABULATED DATA[a]

Hub Drag Reduction Test Data Summary

Langley 14- by 22-Foot Wind Tunnel

June 8, 1988

[a] Note: Some runs were used for weight taring; the data from these runs are not included in this data set.

Run# 40 Test Section Temperature = 81.3 [F] Density = 0.002217 [slug/ft^3]
Reynolds Number/ft= 0.1094370E+07 Static Pressure= 2060.59 [lb/ft^2]

Dynamic Pressure (psf)	Angle of Attack (deg)	C_L	C_D	C_PM	C_RM	C_YM	C_SF
39.99	-1.99	-0.00986	0.11776	-0.57729	0.01711	-0.11899	-0.01054
59.98	-2.12	-0.01987	0.11235	-0.58630	0.01702	-0.12270	-0.00931
79.98	-1.97	-0.01448	0.10826	-0.57504	0.01877	-0.12757	-0.01175
100.20	-1.99	0.00610	0.10727	-0.57281	0.01711	-0.12989	-0.00886
119.62	-2.02	-0.00078	0.10685	-0.58079	0.02174	-0.13374	-0.01486

Run# 41 Test Section Temperature = 71.1 [F] Density = 0.002256 [slug/ft^3]
Reynolds Number/ft= 0.1122261E+07 Static Pressure= 2057.49 [lb/ft^2]

Dynamic Pressure (psf)	Angle of Attack (deg)	C_L	C_D	C_PM	C_RM	C_YM	C_SF
40.12	-2.04	0.07915	0.12575	-0.52070	0.00210	-0.14361	-0.01492
60.24	-2.06	0.05838	0.12463	-0.52840	0.00672	-0.15169	-0.02090
80.36	-2.02	0.05781	0.12268	-0.52832	0.01134	-0.15713	-0.02926
100.82	-2.02	0.05119	0.12275	-0.52705	0.01467	-0.16414	-0.03582
120.36	-2.05	0.05206	0.12221	-0.53086	0.01674	-0.17297	-0.04174

Reference Area = 1.43 ft^2 ; Reference Length = 1.26 ft

Run# 101 Test Section Temperature = 87.5 [F] Density = 0.002160 [slug/ft^3]
Reynolds Number/ft= 0.1515417E+07 Static Pressure= 2019.22 [lb/ft^2]

Dynamic Pressure (psf)	Angle of Attack (deg)	C_L	C_D	C_PM	C_RM	C_YM	C_SF
80.09	2.02	0.01274	0.10888	-0.28782	0.01620	-0.11518	-0.02029
79.98	0.08	0.00306	0.10784	-0.43085	0.01802	-0.11900	-0.01686
79.86	-2.01	-0.01416	0.11012	-0.57767	0.01651	-0.13169	-0.00765
79.98	-4.01	-0.02141	0.10970	-0.71030	0.02602	-0.14108	-0.01227
80.09	-6.01	-0.02611	0.11193	-0.84161	0.02695	-0.14490	-0.00661
79.98	-7.99	-0.04556	0.11394	-0.96641	0.03157	-0.14904	-0.00773
80.09	-10.05	-0.07018	0.11725	-1.08042	0.03644	-0.14987	-0.00773

Run# 103 Test Section Temperature = 80.5 [F] Density = 0.002186 [slug/ft^3]
Reynolds Number/ft= 0.1542266E+07 Static Pressure= 2018.33 [lb/ft^2]

Dynamic Pressure (psf)	Angle of Attack (deg)	C_L	C_D	C_PM	C_RM	C_YM	C_SF
80.36	2.01	0.13736	0.23924	-0.30450	0.00978	-0.11470	-0.01833
80.36	0.01	0.11800	0.23759	-0.43870	0.00805	-0.12615	-0.00669
80.36	-2.02	0.08808	0.23561	-0.56956	0.00782	-0.14112	-0.00126
80.13	-4.01	0.05942	0.23559	-0.68670	0.00990	-0.15813	0.00680
80.01	-6.01	0.03283	0.23527	-0.80138	0.01628	-0.16151	0.00478
80.01	-8.02	0.00132	0.23675	-0.91284	0.02045	-0.16348	0.00438
80.01	-10.02	-0.04113	0.23697	-1.00858	0.02681	-0.16358	0.00314

Reference Area = 1.43 ft^2 ; Reference Length = 1.26 ft

Run# 104 Test Section Temperature = 80.4 [F] Density = 0.002186 [slug/ft^3]
Reynolds Number/ft= 0.1543665E+07 Static Pressure= 2016.22 [lb/ft^2]

Dynamic Pressure (psf)	Angle of Attack (deg)	C_L	C_D	C_PM	C_RM	C_YM	C_SF
80.47	2.02	0.29513	0.23592	-0.31136	0.00638	-0.12425	-0.00945
80.36	-0.04	0.24448	0.22943	-0.45282	0.00663	-0.13207	-0.00392
80.36	-2.02	0.20073	0.22567	-0.58187	0.00481	-0.14780	0.00720
80.24	-4.04	0.15452	0.22145	-0.70469	0.00991	-0.16197	0.00815
80.13	-6.00	0.11011	0.22191	-0.82033	0.01735	-0.16520	0.00597
79.90	-8.05	0.05372	0.22518	-0.93819	0.02285	-0.17163	0.00749
80.01	-10.02	-0.01202	0.22939	-1.03705	0.02872	-0.16840	0.00376

Run# 105 Test Section Temperature = 80.7 [F] Density = 0.002185 [slug/ft^3]
Reynolds Number/ft= 0.1539098E+07 Static Pressure= 2016.56 [lb/ft^2]

Dynamic Pressure (psf)	Angle of Attack (deg)	C_L	C_D	C_PM	C_RM	C_YM	C_SF
80.13	2.09	0.20370	0.23784	-0.26022	0.00778	-0.10842	-0.01301
80.13	0.01	0.14018	0.23587	-0.41117	0.01115	-0.12858	-0.01123
79.90	-2.00	0.10371	0.23327	-0.54328	0.01149	-0.14393	-0.00355
79.78	-4.00	0.05792	0.23337	-0.66913	0.01446	-0.16211	0.00112
80.01	-6.00	0.02300	0.23346	-0.79320	0.01750	-0.16853	0.00506
79.90	-8.05	-0.01241	0.23484	-0.91119	0.02446	-0.16854	0.00284
80.13	-10.04	-0.07275	0.23799	-1.01529	0.03045	-0.16834	0.00034

Reference Area = 1.43 ft^2 ; Reference Length = 1.26 ft

Run# 106 Test Section Temperature = 79.4 [F] Density = 0.002191 [slug/ft^3]
Reynolds Number/ft= 0.1547554E+07 Static Pressure= 2018.85 [lb/ft^2]

Dynamic Pressure (psf)	Angle of Attack (deg)	C_L	C_D	C_PM	C_RM	C_YM	C_SF
80.47	2.06	0.23190	0.23451	-0.27504	-0.00100	-0.11739	-0.00141
80.47	-0.02	0.17959	0.23149	-0.42420	0.00318	-0.12925	-0.00094
80.36	-2.00	0.13017	0.22780	-0.55824	0.00593	-0.14778	0.00475
80.24	-4.00	0.09686	0.22835	-0.68237	0.00967	-0.16168	0.00904
80.13	-6.01	0.06834	0.22669	-0.80221	0.01039	-0.16119	0.01166
80.13	-8.18	0.01693	0.22779	-0.92922	0.01719	-0.16631	0.01144
80.24	-10.00	-0.04684	0.23202	-1.02178	0.02715	-0.16975	0.00430

Run# 107 Test Section Temperature = 73.9 [F] Density = 0.002212 [slug/ft^3]
Reynolds Number/ft= 0.1567389E+07 Static Pressure= 2015.86 [lb/ft^2]

Dynamic Pressure (psf)	Angle of Attack (deg)	C_L	C_D	C_PM	C_RM	C_YM	C_SF
80.47	2.09	0.26074	0.23511	-0.29506	0.00637	-0.12920	-0.00961
80.36	0.00	0.21302	0.23126	-0.44152	0.00788	-0.13344	-0.00477
80.24	-2.03	0.16072	0.22648	-0.57295	0.01062	-0.14835	-0.00267
80.13	-4.07	0.11651	0.22718	-0.70111	0.01518	-0.16271	0.00121
79.90	-6.00	0.07935	0.22304	-0.81484	0.02201	-0.16626	-0.00037
79.78	-8.00	0.04017	0.22322	-0.92811	0.02365	-0.17094	0.00510
79.90	-10.00	-0.02059	0.22954	-1.03152	0.02671	-0.16730	0.00450

Reference Area = 1.43 ft^2 ; Reference Length = 1.26 ft

Run# 108 Test Section Temperature = 73.6 [F] Density = 0.002213 [slug/ft^3]
Reynolds Number/ft= 0.1570563E+07 Static Pressure= 2015.71 [lb/ft^2]

Dynamic Pressure (psf)	Angle of Attack (deg)	C_L	C_D	C_PM	C_RM	C_YM	C_SF
80.70	2.09	0.22730	0.23852	-0.29379	-0.00134	-0.12444	-0.00020
80.24	-0.01	0.18183	0.23392	-0.44333	0.00432	-0.13532	0.00012
80.24	-2.08	0.14065	0.23104	-0.57834	0.00491	-0.14800	0.00781
80.24	-4.00	0.11415	0.22474	-0.69361	0.01067	-0.16095	0.00751
80.01	-6.00	0.07867	0.22300	-0.81352	0.01229	-0.16434	0.00909
80.01	-8.01	0.04047	0.22309	-0.92550	0.01771	-0.16909	0.01197
80.01	-10.00	-0.01648	0.22197	-1.02738	0.02620	-0.17002	0.00695

Run# 109 Test Section Temperature = 77.6 [F] Density = 0.002197 [slug/ft^3]
Reynolds Number/ft= 0.1550287E+07 Static Pressure= 2016.70 [lb/ft^2]

Dynamic Pressure (psf)	Angle of Attack (deg)	C_L	C_D	C_PM	C_RM	C_YM	C_SF
80.13	2.06	0.14008	0.12579	-0.24919	0.01178	-0.12460	-0.05646
80.13	-0.02	0.10055	0.12407	-0.39247	0.00918	-0.13692	-0.03940
80.13	-2.02	0.05745	0.12444	-0.52787	0.01170	-0.15675	-0.03055
79.90	-4.06	0.01179	0.12529	-0.65528	0.01521	-0.17355	-0.02701
79.78	-6.01	-0.00990	0.12462	-0.76825	0.01641	-0.18068	-0.03148
79.78	-8.03	-0.05790	0.12991	-0.88436	0.01991	-0.19552	-0.03062
79.78	-10.10	-0.11730	0.13676	-0.99343	0.02504	-0.19947	-0.03671

Reference Area = 1.43 ft^2 ; Reference Length = 1.26 ft

Run# 110 Test Section Temperature = 75.3 [F] Density = 0.002207 [slug/ft^3]
Reynolds Number/ft= 0.1557819E+07 Static Pressure= 2016.96 [lb/ft^2]

Dynamic Pressure (psf)	Angle of Attack (deg)	C_L	C_D	C_PM	C_RM	C_YM	C_SF
80.01	2.02	0.04903	0.13851	-0.27421	0.00883	-0.13467	0.01461
79.90	0.00	0.03331	0.14017	-0.40406	0.00769	-0.13317	0.02840
80.01	-1.99	0.00998	0.14520	-0.53348	0.00879	-0.14601	0.04057
79.67	-4.01	-0.01995	0.14843	-0.65223	0.01841	-0.15487	0.03617
80.24	-6.01	-0.03896	0.15308	-0.76555	0.02774	-0.15850	0.02509
80.24	-8.05	-0.07599	0.15900	-0.88134	0.03210	-0.16595	0.02362
80.24	-10.09	-0.09473	0.16225	-0.97843	0.03260	-0.17032	0.01603

Run# 111 Test Section Temperature = 76.2 [F] Density = 0.002202 [slug/ft^3]
Reynolds Number/ft= 0.1556280E+07 Static Pressure= 2016.17 [lb/ft^2]

Dynamic Pressure (psf)	Angle of Attack (deg)	C_L	C_D	C_PM	C_RM	C_YM	C_SF
80.24	2.06	0.04969	0.13643	-0.26818	0.01358	-0.13107	0.00922
80.13	0.01	0.03081	0.13879	-0.40449	0.01271	-0.13362	0.01622
80.13	-2.00	0.01139	0.14098	-0.53351	0.01381	-0.15075	0.02463
79.90	-4.00	-0.02335	0.14031	-0.64934	0.02178	-0.16056	0.02070
80.24	-6.02	-0.04620	0.14620	-0.76835	0.03173	-0.16321	0.00724
80.13	-8.02	-0.06287	0.15055	-0.87675	0.03077	-0.16976	0.01005
80.24	-10.04	-0.10001	0.15754	-0.97773	0.03694	-0.17140	0.00255

Reference Area = 1.43 ft^2 ; Reference Length = 1.26 ft

Run# 112 Test Section Temperature = 75.7 [F] Density = 0.002203 [slug/ft^3]
Reynolds Number/ft= 0.1556900E+07 Static Pressure= 2015.71 [lb/ft^2]

Dynamic Pressure (psf)	Angle of Attack (deg)	C_L	C_D	C_PM	C_RM	C_YM	C_SF
80.13	2.06	0.07761	0.12664	-0.26321	0.01272	-0.12552	-0.03600
80.01	0.00	0.03735	0.13067	-0.40600	0.01638	-0.14177	-0.02405
80.01	-2.03	0.00311	0.13093	-0.53835	0.01648	-0.16380	-0.01263
80.36	-4.01	-0.00940	0.13124	-0.64932	0.01428	-0.17526	-0.00412
80.24	-6.01	-0.04573	0.13254	-0.77002	0.02754	-0.18310	-0.02206
80.24	-8.01	-0.07565	0.13826	-0.88126	0.02963	-0.19879	-0.02268
80.47	-10.00	-0.11438	0.14389	-0.98102	0.03335	-0.20108	-0.02735

Run# 113 Test Section Temperature = 77.0 [F] Density = 0.002205 [slug/ft^3]
Reynolds Number/ft= 0.1555703E+07 Static Pressure= 2020.97 [lb/ft^2]

Dynamic Pressure (psf)	Angle of Attack (deg)	C_L	C_D	C_PM	C_RM	C_YM	C_SF
80.24	2.01	0.11072	0.17910	-0.25287	0.00773	-0.12169	-0.00695
80.01	0.04	0.07917	0.17957	-0.38146	0.00750	-0.13094	-0.00028
79.78	-2.01	0.05716	0.17852	-0.51258	0.01000	-0.14545	0.00694
80.24	-4.03	0.02138	0.17472	-0.62793	0.01489	-0.16231	0.00869
79.90	-6.01	-0.00605	0.18208	-0.74486	0.01814	-0.16936	0.00224
80.13	-8.03	-0.03277	0.18297	-0.85964	0.02405	-0.17728	-0.00559
80.01	-10.01	-0.06893	0.18677	-0.95765	0.03066	-0.18680	-0.00868

Reference Area = 1.43 ft^2 ; Reference Length = 1.28 ft

Run# 114 Test Section Temperature = 82.4 [F] Density = 0.002185 [slug/ft^3]
Reynolds Number/ft= 0.1533367E+07 Static Pressure= 2021.81 [lb/ft^2]

Dynamic Pressure (psf)	Angle of Attack (deg)	C_L	C_D	C_PM	C_RM	C_YM	C_SF
79.90	2.06	0.15276	0.18024	-0.22437	0.01084	-0.12628	-0.06524
79.78	0.01	0.10170	0.17596	-0.36538	0.01179	-0.13938	-0.05908
80.13	-2.05	0.05720	0.16992	-0.49956	0.00848	-0.16727	-0.04637
79.78	-4.00	0.02409	0.16869	-0.62130	0.01244	-0.17867	-0.03330
79.90	-6.06	-0.01120	0.17139	-0.74219	0.01373	-0.18184	-0.03335
80.01	-7.99	-0.05503	0.17181	-0.85065	0.02161	-0.19865	-0.02841
80.01	-10.03	-0.10700	0.18081	-0.96088	0.02604	-0.18924	-0.02855

Run# 115 Test Section Temperature = 79.7 [F] Density = 0.002198 [slug/ft^3]
Reynolds Number/ft= 0.1545588E+07 Static Pressure= 2022.65 [lb/ft^2]

Dynamic Pressure (psf)	Angle of Attack (deg)	C_L	C_D	C_PM	C_RM	C_YM	C_SF
80.13	2.04	0.15430	0.17111	-0.23345	0.00855	-0.12198	-0.05788
80.24	0.02	0.10973	0.16582	-0.37007	0.00799	-0.13414	-0.05619
80.13	-2.01	0.08357	0.16619	-0.50115	0.00739	-0.15565	-0.02750
80.01	-4.02	0.03210	0.16451	-0.62779	0.01357	-0.16939	-0.02483
79.90	-6.04	-0.01457	0.16609	-0.74698	0.02105	-0.18285	-0.02410
79.90	-8.02	-0.05555	0.16733	-0.86016	0.01972	-0.18449	-0.01967
80.24	-10.05	-0.10824	0.16765	-0.97022	0.02491	-0.21541	-0.04797

Reference Area = 1.43 ft^2 ; Reference Length = 1.26 ft

Run# 116 Test Section Temperature = 80.5 [F] Density = 0.002193 [slug/ft^3]
Reynolds Number/ft= 0.1544804E+07 Static Pressure= 2023.19 [lb/ft^2]

Dynamic Pressure (psf)	Angle of Attack (deg)	C_L	C_D	C_PM	C_RM	C_YM	C_SF
80.36	2.01	0.16234	0.16741	-0.24127	0.01367	-0.12573	-0.04633
80.47	-0.01	0.13627	0.16427	-0.37759	0.01041	-0.13846	-0.02992
80.24	-2.04	0.08740	0.15937	-0.51530	0.01993	-0.16121	-0.02920
80.01	-4.08	0.05753	0.15825	-0.63498	0.01242	-0.17978	-0.01082
80.13	-6.01	0.01149	0.15997	-0.75231	0.02494	-0.19456	-0.01946
80.01	-8.01	-0.02621	0.16360	-0.86524	0.02756	-0.20663	-0.02246
80.13	-10.02	-0.07853	0.17033	-0.96816	0.03193	-0.21562	-0.02186

Run# 117 Test Section Temperature = 78.2 [F] Density = 0.002205 [slug/ft^3]
Reynolds Number/ft= 0.1554114E+07 Static Pressure= 2024.68 [lb/ft^2]

Dynamic Pressure (psf)	Angle of Attack (deg)	C_L	C_D	C_PM	C_RM	C_YM	C_SF
80.36	2.07	0.11371	0.14259	-0.25463	-0.00439	-0.13634	0.03817
80.24	-0.05	0.07222	0.14336	-0.39374	-0.00022	-0.15085	0.03463
80.47	-2.02	0.03583	0.13803	-0.51772	0.00761	-0.15863	0.03139
80.36	-4.03	-0.00115	0.13822	-0.64297	0.00997	-0.16607	0.02930
80.24	-6.10	-0.04423	0.14005	-0.76290	0.02099	-0.15999	0.01538
80.13	-8.01	-0.07747	0.14350	-0.86877	0.02476	-0.16297	0.01441
80.36	-10.02	-0.12115	0.15175	-0.97446	0.02890	-0.16363	0.00151

Reference Area = 1.43 ft^2 ; Reference Length = 1.26 ft

Run# 118 Test Section Temperature = 75.5 [F] Density = 0.002217 [slug/ft^3]
Reynolds Number/ft= 0.1558751E+07 Static Pressure= 2025.47 [lb/ft^2]

Dynamic Pressure (psf)	Angle of Attack (deg)	C_L	C_D	C_PM	C_RM	C_YM	C_SF
79.78	2.07	0.12962	0.14509	-0.25408	0.00588	-0.11708	-0.03621
79.90	-0.01	0.10272	0.14284	-0.39277	0.00503	-0.12402	-0.02750
79.67	-2.08	0.06880	0.13677	-0.52688	0.00932	-0.15074	-0.01438
80.13	-4.00	0.01097	0.13742	-0.64513	0.01528	-0.17073	-0.00660
80.13	-6.01	-0.03085	0.13359	-0.75766	0.01746	-0.17550	-0.01448
80.13	-8.02	-0.07384	0.13933	-0.87620	0.02181	-0.18179	-0.02275
80.01	-10.02	-0.12717	0.14852	-0.98339	0.02342	-0.18828	-0.02621

Run# 119 Test Section Temperature = 71.0 [F] Density = 0.002235 [slug/ft^3]
Reynolds Number/ft= 0.1578649E+07 Static Pressure= 2025.47 [lb/ft^2]

Dynamic Pressure (psf)	Angle of Attack (deg)	C_L	C_D	C_PM	C_RM	C_YM	C_SF
80.13	2.05	0.16182	0.18118	-0.25592	0.01643	-0.13807	0.03004
80.13	0.02	0.12527	0.17320	-0.39092	0.01876	-0.14709	0.02139
80.13	-2.06	0.08092	0.15740	-0.52531	0.00983	-0.16134	0.01169
80.13	-4.11	0.02615	0.15567	-0.64581	0.01362	-0.17612	0.00875
79.90	-6.08	-0.00877	0.15613	-0.76367	0.02733	-0.17023	-0.00381
79.90	-8.07	-0.05567	0.15903	-0.87367	0.02685	-0.17340	-0.00391
80.13	-10.03	-0.10881	0.16746	-0.97452	0.02716	-0.17629	-0.00260

Reference Area = 1.43 ft^2 ; Reference Length = 1.26 ft

Run# 120 Test Section Temperature = 68.6 [F] Density = 0.002251 [slug/ft^3]
Reynolds Number/ft= 0.1588516E+07 Static Pressure= 2030.75 [lb/ft^2]

Dynamic Pressure (psf)	Angle of Attack (deg)	C_L	C_D	C_PM	C_RM	C_YM	C_SF
80.01	2.03	0.08602	0.17559	-0.24923	0.01532	-0.12905	-0.04290
80.01	0.01	0.06402	0.17395	-0.38411	0.00705	-0.13570	-0.02502
80.59	-2.06	0.03757	0.17001	-0.51307	0.00960	-0.15441	-0.01710
80.24	-4.03	0.01675	0.17117	-0.62884	0.01033	-0.16564	-0.00786
80.36	-6.02	-0.03245	0.17391	-0.74268	0.02406	-0.17200	-0.01764
80.24	-8.00	-0.04455	0.17689	-0.85123	0.02472	-0.16480	-0.00361
80.24	-10.12	-0.08644	0.18316	-0.95779	0.03030	-0.15803	0.00367

Run# 121 Test Section Temperature = 70.4 [F] Density = 0.002243 [slug/ft^3]
Reynolds Number/ft= 0.1581814E+07 Static Pressure= 2030.81 [lb/ft^2]

Dynamic Pressure (psf)	Angle of Attack (deg)	C_L	C_D	C_PM	C_RM	C_YM	C_SF
80.01	2.05	0.19063	0.15343	-0.24864	0.00124	-0.12938	0.01169
80.13	0.00	0.13878	0.15083	-0.38750	0.00610	-0.13630	0.01001
80.24	-2.05	0.10110	0.14653	-0.52127	0.00739	-0.15107	0.01811
79.90	-4.03	0.06831	0.14763	-0.63906	0.00786	-0.16220	0.02483
79.78	-6.02	0.02257	0.14707	-0.75858	0.01453	-0.16841	0.01540
80.13	-8.03	-0.00732	0.14850	-0.86938	0.02001	-0.16979	0.01186
80.13	-10.03	-0.08209	0.15821	-0.97528	0.03308	-0.17149	-0.00031

Reference Area = 1.43 ft^2 ; Reference Length = 1.26 ft

Run# 122 Test Section Temperature = 73.0 [F] Density = 0.002245 [slug/ft^3]
Reynolds Number/ft= 0.1577454E+07 Static Pressure= 2040.33 [lb/ft^2]

Dynamic Pressure (psf)	Angle of Attack (deg)	C_L	C_D	C_PM	C_RM	C_YM	C_SF
80.13	2.06	0.21339	0.17759	-0.24388	0.00436	-0.12106	-0.00953
79.90	0.00	0.17349	0.17209	-0.38471	0.00509	-0.13124	-0.00328
80.24	-2.02	0.14549	0.16956	-0.51424	0.00410	-0.14396	0.01154
79.90	-3.99	0.09848	0.16754	-0.63058	0.00863	-0.16762	0.01418
80.13	-6.04	0.04158	0.16623	-0.75527	0.02118	-0.17420	-0.00037
80.13	-8.01	0.01058	0.17057	-0.86859	0.02583	-0.17999	0.00009
79.90	-10.01	-0.05344	0.17848	-0.97256	0.03179	-0.18062	-0.00618

Run# 123 Test Section Temperature = 77.5 [F] Density = 0.002227 [slug/ft^3]
Reynolds Number/ft= 0.1558889E+07 Static Pressure= 2040.70 [lb/ft^2]

Dynamic Pressure (psf)	Angle of Attack (deg)	C_L	C_D	C_PM	C_RM	C_YM	C_SF
79.90	2.03	0.10536	0.18407	-0.24644	0.01013	-0.12465	-0.03354
79.90	0.01	0.08690	0.18304	-0.38023	0.00869	-0.13713	-0.02038
80.13	-1.99	0.05454	0.17871	-0.50592	0.01025	-0.14917	-0.01452
80.01	-4.01	0.01696	0.17939	-0.62585	0.01499	-0.16437	-0.00807
79.90	-6.05	0.00012	0.17764	-0.73647	0.01643	-0.16911	-0.00471
80.13	-8.01	-0.03860	0.18159	-0.85040	0.02546	-0.16771	-0.01057
80.13	-10.04	-0.06717	0.18561	-0.95075	0.02922	-0.16022	-0.00204

Reference Area = 1.43 ft^2 ; Reference Length = 1.26 ft

Run# 124 Test Section Temperature = 78.6 [F] Density = 0.002231 [slug/ft^3]
Reynolds Number/ft= 0.1563473E+07 Static Pressure= 2040.66 [lb/ft^2]

Dynamic Pressure (psf)	Angle of Attack (deg)	C_L	C_D	C_PM	C_RM	C_YM	C_SF
80.01	2.00	0.10478	0.18046	-0.24881	0.01164	-0.12712	-0.03594
80.13	0.07	0.08409	0.17937	-0.37653	0.01086	-0.13232	-0.02947
80.13	-2.02	0.05363	0.17764	-0.50792	0.01225	-0.14889	-0.02248
79.67	-4.01	0.01638	0.18165	-0.62628	0.01723	-0.16857	-0.01907
80.01	-6.02	-0.01383	0.18218	-0.74092	0.02030	-0.17247	-0.02269
80.13	-8.03	-0.04104	0.18502	-0.85256	0.02864	-0.18221	-0.02427
80.24	-10.04	-0.07145	0.19021	-0.95200	0.02865	-0.17265	-0.01675

Run# 125 Test Section Temperature = 81.0 [F] Density = 0.002213 [slug/ft^3]
Reynolds Number/ft= 0.1548640E+07 Static Pressure= 2040.89 [lb/ft^2]

Dynamic Pressure (psf)	Angle of Attack (deg)	C_L	C_D	C_PM	C_RM	C_YM	C_SF
80.13	2.06	0.21560	0.18222	-0.24185	0.01064	-0.12408	-0.02763
79.90	-0.04	0.18438	0.17913	-0.38712	0.00811	-0.13116	-0.01458
80.13	-2.00	0.13333	0.17666	-0.51828	0.01425	-0.15260	-0.00717
80.01	-4.06	0.09560	0.17260	-0.63817	0.01663	-0.16917	0.00118
80.24	-6.00	0.05994	0.17142	-0.75357	0.01924	-0.16745	-0.00396
80.24	-8.03	0.00874	0.17816	-0.87298	0.02741	-0.17979	-0.00381
80.24	-10.08	-0.04796	0.17716	-0.97435	0.03522	-0.17501	-0.01073

Reference Area = 1.43 ft^2 ; Reference Length = 1.26 ft

Run# 126 Test Section Temperature = 77.2 [F] Density = 0.002228 [slug/ft^3]
Reynolds Number/ft= 0.1562191E+07 Static Pressure= 2040.26 [lb/ft^2]

Dynamic Pressure (psf)	Angle of Attack (deg)	C_L	C_D	C_PM	C_RM	C_YM	C_SF
80.13	2.08	0.24044	0.19095	-0.23850	0.00194	-0.11983	-0.01178
80.01	0.00	0.18676	0.18459	-0.38289	0.00180	-0.13142	-0.00636
80.13	-2.06	0.14179	0.18003	-0.51899	0.01085	-0.15210	-0.00382
80.24	-4.02	0.09623	0.17706	-0.63305	0.00982	-0.17515	0.00363
80.13	-6.04	0.05593	0.17914	-0.75659	0.02313	-0.17975	-0.00466
80.24	-8.06	0.01147	0.18125	-0.87301	0.02677	-0.18566	-0.00431
80.01	-10.03	-0.04963	0.18106	-0.97313	0.03317	-0.18502	-0.00917

Run# 127 Test Section Temperature = 82.1 [F] Density = 0.002208 [slug/ft^3]
Reynolds Number/ft= 0.1542070E+07 Static Pressure= 2040.06 [lb/ft^2]

Dynamic Pressure (psf)	Angle of Attack (deg)	C_L	C_D	C_PM	C_RM	C_YM	C_SF
79.90	2.01	0.08653	0.17599	-0.24878	0.01402	-0.12949	-0.04511
80.13	0.05	0.06236	0.17904	-0.38008	0.01296	-0.13623	-0.03496
80.01	-2.05	0.04529	0.18041	-0.51232	0.00728	-0.15360	-0.02094
80.01	-4.03	0.01111	0.17919	-0.62610	0.01383	-0.16998	-0.01461
80.13	-6.00	-0.01785	0.18506	-0.74317	0.01747	-0.17416	-0.02111
80.01	-8.03	-0.04875	0.18621	-0.85143	0.02287	-0.17852	-0.02462
80.01	-10.03	-0.08372	0.19363	-0.95349	0.03175	-0.17321	-0.02294

Reference Area = 1.43 ft^2 : Reference Length = 1.26 ft

Run# 133 Test Section Temperature = 84.0 [F] Density = 0.002199 [slug/ft^3]
Reynolds Number/ft= 0.1536872E+07 Static Pressure= 2039.13 [lb/ft^2]

Dynamic Pressure (psf)	Angle of Attack (deg)	C_L	C_D	C_PM	C_RM	C_YM	C_SF
80.13	2.10	0.20301	0.20847	-0.21739	0.00575	-0.12213	-0.02491
80.13	0.06	0.16726	0.20280	-0.35537	0.00636	-0.12901	-0.01031
80.13	-1.99	0.11765	0.19831	-0.48970	0.01177	-0.13511	-0.00595
80.13	-4.04	0.06807	0.19444	-0.60774	0.01465	-0.15290	-0.00075
79.90	-6.03	0.02149	0.19993	-0.71947	0.01753	-0.15518	-0.00484
80.13	-8.03	-0.02298	0.19954	-0.83113	0.02033	-0.15704	-0.00947
80.01	-9.99	-0.08074	0.20683	-0.93117	0.02442	-0.15517	-0.01492

Run# 134 Test Section Temperature = 83.1 [F] Density = 0.002202 [slug/ft^3]
Reynolds Number/ft= 0.1542295E+07 Static Pressure= 2038.82 [lb/ft^2]

Dynamic Pressure (psf)	Angle of Attack (deg)	C_L	C_D	C_PM	C_RM	C_YM	C_SF
80.36	1.99	0.17067	0.21295	-0.19802	0.01142	-0.12546	-0.03455
80.13	-0.05	0.12717	0.21523	-0.33723	0.01139	-0.13325	-0.02164
79.78	-2.00	0.07911	0.21399	-0.45904	0.01095	-0.14688	-0.00802
80.01	-4.00	0.02954	0.20663	-0.57164	0.01306	-0.15330	-0.00233
80.13	-6.05	-0.02359	0.21259	-0.68530	0.01901	-0.16381	-0.00754
80.13	-8.03	-0.06951	0.21645	-0.79507	0.02180	-0.16244	-0.01170
80.13	-10.09	-0.12510	0.22542	-0.89859	0.02610	-0.15354	-0.01935

Reference Area = 1.43 ft^2 . Reference Length = 1.26 ft

Run# 135 Test Section Temperature = 84.8 [F] Density = 0.002195 [slug/ft^3]
Reynolds Number/ft= 0.1531824E+07 Static Pressure= 2039.14 [lb/ft^2]

Dynamic Pressure (psf)	Angle of Attack (deg)	C_L	C_D	C_PM	C_RM	C_YM	C_SF
79.90	2.01	0.08902	0.19068	-0.24426	0.00903	-0.12828	-0.04285
80.24	-0.02	0.04974	0.18992	-0.37020	0.00841	-0.14286	-0.03422
80.36	-2.01	0.02932	0.19290	-0.48493	0.00553	-0.15487	-0.01527
80.13	-4.05	-0.02542	0.19976	-0.60492	0.01696	-0.16721	-0.01997
79.90	-5.99	-0.04412	0.20291	-0.71027	0.01427	-0.17032	-0.01352
80.13	-8.01	-0.09468	0.21505	-0.81769	0.02019	-0.17570	-0.02132
80.24	-10.06	-0.13396	0.22141	-0.91409	0.02462	-0.16626	-0.02765

Run# 136 Test Section Temperature = 79.4 [F] Density = 0.002217 [slug/ft^3]
Reynolds Number/ft= 0.1554625E+07 Static Pressure= 2038.94 [lb/ft^2]

Dynamic Pressure (psf)	Angle of Attack (deg)	C_L	C_D	C_PM	C_RM	C_YM	C_SF
80.24	2.01	0.11450	0.11840	-0.25405	0.01239	-0.12645	-0.04469
80.24	0.01	0.08689	0.11866	-0.38919	0.01036	-0.13647	-0.03127
80.24	-2.03	0.05049	0.11698	-0.52598	0.00976	-0.15623	-0.02055
80.24	-4.03	0.00805	0.11800	-0.64592	0.01133	-0.16915	-0.01468
80.13	-6.03	-0.02188	0.11990	-0.76240	0.01105	-0.17202	-0.01315
80.13	-8.01	-0.07424	0.12654	-0.87711	0.02348	-0.18108	-0.01969
80.13	-10.01	-0.12146	0.13434	-0.97683	0.02387	-0.18207	-0.02172

Reference Area = 1.43 ft^2 : Reference Length = 1.26 ft

Run# 137 Test Section Temperature = 78.0 [F] Density = 0.002222 [slug/ft^3]
Reynolds Number/ft= 0.1560554E+07 Static Pressure= 2038.68 [lb/ft^2]

Dynamic Pressure (psf)	Angle of Attack (deg)	C_L	C_D	C_PM	C_RM	C_YM	C_SF
80.36	2.05	0.04850	0.11934	-0.25351	0.00746	-0.11810	-0.04091
80.24	0.01	0.01475	0.12762	-0.39290	0.00978	-0.12816	-0.03560
80.24	-2.00	-0.00785	0.13053	-0.52278	0.00934	-0.14920	-0.02351
80.13	-4.02	-0.02985	0.13047	-0.64098	0.01209	-0.16258	-0.01590
80.01	-6.02	-0.05609	0.13256	-0.75269	0.01731	-0.17204	-0.02240
80.13	-8.00	-0.08237	0.13929	-0.86592	0.02114	-0.17807	-0.02277
80.24	-10.00	-0.11533	0.14382	-0.96550	0.02666	-0.17771	-0.02673

Run# 140 Test Section Temperature = 82.6 [F] Density = 0.002203 [slug/ft^3]
Reynolds Number/ft= 0.1541451E+07 Static Pressure= 2038.14 [lb/ft^2]

Dynamic Pressure (psf)	Angle of Attack (deg)	C_L	C_D	C_PM	C_RM	C_YM	C_SF
80.13	2.02	0.08845	0.19975	-0.24305	0.00851	-0.12039	-0.02916
80.13	-0.01	0.06242	0.20225	-0.38098	0.00731	-0.12419	-0.02007
80.13	-2.07	0.05897	0.21250	-0.52109	0.00716	-0.14887	-0.00689
80.13	-4.00	0.02829	0.21408	-0.63822	0.01191	-0.16129	-0.00628
79.90	-6.02	0.00429	0.21333	-0.76017	0.01975	-0.16815	-0.01113
79.90	-8.03	-0.02693	0.21950	-0.87735	0.02293	-0.17532	-0.00998
80.01	-10.01	-0.06961	0.22559	-0.97472	0.02729	-0.17781	-0.01333
80.13	-2.01	0.06083	0.21075	-0.51519	0.00812	-0.14608	-0.00764
80.13	-0.01	0.07582	0.20575	-0.38154	0.00816	-0.13131	-0.01916

Reference Area = 1.43 ft^2 ; Reference Length = 1.26 ft

Run# 141 Test Section Temperature = 83.8 [F] Density = 0.002198 [slug/ft^3]
Reynolds Number/ft= 0.1537328E+07 Static Pressure= 2038.28 [lb/ft^2]

Dynamic Pressure (psf)	Angle of Attack (deg)	C_L	C_D	C_PM	C_RM	C_YM	C_SF
80.13	2.00	0.22691	0.21187	-0.25905	0.01106	-0.12291	-0.02682
80.01	0.00	0.19703	0.20836	-0.40007	0.00789	-0.13390	-0.01683
80.13	-2.00	0.15804	0.20587	-0.53285	0.00925	-0.15312	-0.00733
80.24	-4.05	0.10284	0.20430	-0.66075	0.01894	-0.16808	-0.01031
80.13	-6.02	0.04101	0.20250	-0.77553	0.02231	-0.17802	-0.00919
79.90	-8.02	-0.01016	0.20884	-0.89216	0.02311	-0.18143	-0.00631
80.13	-10.03	-0.07088	0.21397	-0.99552	0.03556	-0.17968	-0.01049

Run# 142 Test Section Temperature = 76.6 [F] Density = 0.002229 [slug/ft^3]
Reynolds Number/ft= 0.1567111E+07 Static Pressure= 2039.20 [lb/ft^2]

Dynamic Pressure (psf)	Angle of Attack (deg)	C_L	C_D	C_PM	C_RM	C_YM	C_SF
80.47	1.99	0.12201	0.11379	-0.25942	0.00924	-0.12431	-0.02710
80.24	0.01	0.08342	0.11247	-0.38655	0.01122	-0.13898	-0.01937
80.13	-2.05	0.05226	0.11354	-0.53343	0.00868	-0.15466	-0.00532
80.24	-4.00	0.00981	0.11642	-0.65112	0.01217	-0.17217	-0.00162
79.90	-6.06	-0.02021	0.11891	-0.77320	0.01821	-0.17926	-0.00479
79.90	-8.02	-0.05803	0.12442	-0.88759	0.02243	-0.18245	-0.00824
80.13	-10.05	-0.11223	0.13197	-0.98882	0.02612	-0.18193	-0.01088

Reference Area = 1.43 ft^2 ; Reference Length = 1.26 ft

Run# 143 Test Section Temperature = 69.7 [F] Density = 0.002260 [slug/ft^3]
Reynolds Number/ft= 0.1580531E+07 Static Pressure= 2041.53 [lb/ft^2]

Dynamic Pressure (psf)	Angle of Attack (deg)	C_L	C_D	C_PM	C_RM	C_YM	C_SF
80.13	2.04	0.13450	0.11572	-0.27137	0.00800	-0.12208	-0.01424
80.01	0.01	0.10757	0.11462	-0.41548	0.00812	-0.12854	-0.00432
79.78	-2.07	0.07727	0.11074	-0.54953	0.00722	-0.14647	0.00258
80.24	-4.02	0.03274	0.11059	-0.67037	0.01268	-0.15987	0.00344
79.78	-6.02	-0.00398	0.11137	-0.79086	0.01660	-0.15779	-0.00063
79.78	-8.11	-0.05210	0.11838	-0.91262	0.02484	-0.16169	-0.00548
80.47	-10.00	-0.09807	0.12357	-1.00577	0.02883	-0.15709	-0.00958

Run# 144 Test Section Temperature = 68.4 [F] Density = 0.002246 [slug/ft^3]
Reynolds Number/ft= 0.1590780E+07 Static Pressure= 2025.60 [lb/ft^2]

Dynamic Pressure (psf)	Angle of Attack (deg)	C_L	C_D	C_PM	C_RM	C_YM	C_SF
80.36	2.02	0.14847	0.12827	-0.24692	0.01049	-0.13594	-0.03840
80.36	0.01	0.10461	0.12826	-0.38560	0.01466	-0.14160	-0.03338
80.36	-2.03	0.04785	0.12813	-0.52754	0.01143	-0.16295	-0.02332
80.24	-4.03	-0.00873	0.12787	-0.65189	0.01534	-0.17818	-0.02068
80.01	-6.06	-0.06553	0.13372	-0.77845	0.02257	-0.16958	-0.02868
80.24	-8.20	-0.12894	0.14260	-0.90267	0.02937	-0.18318	-0.03650
80.01	-10.00	-0.19571	0.15617	-1.00325	0.02818	-0.19089	-0.03310

Reference Area = 1.43 ft^2 ; Reference Length = 1.28 ft

Run# 145 Test Section Temperature = 67.7 [F] Density = 0.002249 [slug/ft^3]
Reynolds Number/ft= 0.1592229E+07 Static Pressure= 2025.43 [lb/ft^2]

Dynamic Pressure (psf)	Angle of Attack (deg)	C_L	C_D	C_PM	C_RM	C_YM	C_SF
80.24	2.05	0.17706	0.13562	-0.22508	0.01113	-0.13125	-0.05107
80.13	0.01	0.12584	0.13001	-0.37555	0.00205	-0.14202	-0.03403
80.13	-2.00	0.07864	0.12661	-0.51616	0.00448	-0.15935	-0.01764
80.01	-4.00	0.00803	0.12655	-0.65173	0.00799	-0.17225	-0.01302
80.13	-6.02	-0.06394	0.13468	-0.78450	0.01381	-0.17049	-0.01812
80.13	-8.00	-0.14325	0.14135	-0.90648	0.02566	-0.18023	-0.02607
80.36	-10.07	-0.22919	0.15648	-1.02803	0.02615	-0.17342	-0.04126

Run# 146 Test Section Temperature = 67.3 [F] Density = 0.002272 [slug/ft^3]
Reynolds Number/ft= 0.1600429E+07 Static Pressure= 2042.94 [lb/ft^2]

Dynamic Pressure (psf)	Angle of Attack (deg)	C_L	C_D	C_PM	C_RM	C_YM	C_SF
80.13	2.00	0.11864	0.11730	-0.24181	0.01327	-0.11308	-0.06516
80.01	0.00	0.08233	0.11631	-0.38318	0.01677	-0.12335	-0.06677
80.13	-2.01	0.04232	0.11563	-0.51660	0.01692	-0.14631	-0.06110
79.90	-4.06	0.00292	0.11735	-0.64333	0.00974	-0.16727	-0.04860
80.01	-6.01	-0.03484	0.12145	-0.76217	0.01629	-0.17493	-0.04777
80.13	-8.02	-0.08935	0.12866	-0.87845	0.02108	-0.19875	-0.04747
80.13	-10.00	-0.14433	0.13621	-0.98984	0.02443	-0.20752	-0.04598

Reference Area = 1.43 ft^2 ; Reference Length = 1.28 ft

Run# 147 Test Section Temperature = 68.8 [F] Density = 0.002285 [slug/ft^3]
Reynolds Number/ft= 0.1596770E+07 Static Pressure= 2042.71 [lb/ft^2]

Dynamic Pressure (psf)	Angle of Attack (deg)	C_L	C_D	C_PM	C_RM	C_YM	C_SF
80.36	2.00	0.19030	0.21036	-0.22694	0.01486	-0.11487	-0.05244
80.13	-0.01	0.15288	0.20679	-0.36570	0.01199	-0.13278	-0.03820
79.90	-2.00	0.11457	0.20416	-0.49197	0.00857	-0.15032	-0.02785
79.90	-4.01	0.06490	0.20376	-0.61720	0.01484	-0.17762	-0.02624
80.01	-6.09	0.02541	0.20311	-0.73985	0.01878	-0.18867	-0.02560
80.01	-8.01	-0.01451	0.20630	-0.85344	0.02596	-0.20748	-0.02212
80.01	-10.01	-0.07774	0.21156	-0.95569	0.03190	-0.21452	-0.01934

Run# 148 Test Section Temperature = 69.2 [F] Density = 0.002284 [slug/ft^3]
Reynolds Number/ft= 0.1595203E+07 Static Pressure= 2042.64 [lb/ft^2]

Dynamic Pressure (psf)	Angle of Attack (deg)	C_L	C_D	C_PM	C_RM	C_YM	C_SF
80.36	2.04	0.24088	0.21463	-0.22993	0.00812	-0.11586	-0.04125
80.13	0.01	0.18905	0.20892	-0.37043	0.01156	-0.13842	-0.03714
80.13	-2.01	0.14692	0.20698	-0.50127	0.00959	-0.17373	-0.02445
80.13	-4.01	0.10843	0.20568	-0.62095	0.01011	-0.19442	-0.01368
80.01	-6.04	0.07108	0.20537	-0.74258	0.01628	-0.20805	-0.01068
79.90	-8.02	0.02234	0.20808	-0.85558	0.02241	-0.21926	-0.01396
80.01	-10.13	-0.03833	0.21568	-0.95898	0.03098	-0.22684	-0.01555

Reference Area = 1.43 ft^2 ; Reference Length = 1.26 ft

Run# 149 Test Section Temperature = 69.7 [F] Density = 0.002262 [slug/ft^3]
Reynolds Number/ft= 0.1593291E+07 Static Pressure= 2042.29 [lb/ft^2]

Dynamic Pressure (psf)	Angle of Attack (deg)	C_L	C_D	C_PM	C_RM	C_YM	C_SF
80.36	2.05	0.16274	0.21078	-0.21885	0.01230	-0.11314	-0.04722
80.13	0.02	0.11667	0.20523	-0.35850	0.00990	-0.12507	-0.03837
80.13	-2.02	0.07308	0.20259	-0.49459	0.01522	-0.14273	-0.03738
80.24	-4.01	0.02881	0.20399	-0.61336	0.01455	-0.16183	-0.03234
80.01	-6.04	-0.00880	0.20541	-0.73557	0.01808	-0.17209	-0.03378
80.01	-8.03	-0.04937	0.20811	-0.85047	0.02205	-0.19388	-0.02539
80.01	-10.00	-0.10300	0.21804	-0.95247	0.02982	-0.20367	-0.02857

Run# 150 Test Section Temperature = 69.5 [F] Density = 0.002262 [slug/ft^3]
Reynolds Number/ft= 0.1592757E+07 Static Pressure= 2041.91 [lb/ft^2]

Dynamic Pressure (psf)	Angle of Attack (deg)	C_L	C_D	C_PM	C_RM	C_YM	C_SF
80.24	2.03	0.15268	0.21228	-0.23238	0.01698	-0.11942	-0.04659
80.24	-0.01	0.12755	0.20813	-0.37497	0.01295	-0.14454	-0.03497
80.36	-2.01	0.10977	0.20675	-0.49898	0.00753	-0.16640	-0.01967
80.24	-4.07	0.07515	0.20598	-0.62344	0.00771	-0.18551	-0.01178
80.01	-6.00	0.03863	0.20726	-0.74147	0.01060	-0.19198	-0.01421
79.90	-8.00	0.00134	0.20949	-0.85376	0.01800	-0.21226	-0.01098
80.24	-10.00	-0.06050	0.21454	-0.95439	0.02697	-0.21820	-0.01598

Reference Area = 1.43 ft^2 : Reference Length = 1.26 ft

Run# 245 Test Section Temperature = 82.1 [F] Density = 0.002204 [slug/ft^3]
Reynolds Number/ft= 0.1543001E+07 Static Pressure= 2037.92 [lb/ft^2]

Dynamic Pressure (psf)	Angle of Attack (deg)	C_L	C_D	C_PM	C_RM	C_YM	C_SF
80.13	-9.99	-0.24075	0.15807	-1.02308	0.03276	-0.18650	-0.04472
80.13	-8.03	-0.14261	0.14304	-0.90488	0.02161	-0.18118	-0.03246
80.13	-6.07	-0.08388	0.13289	-0.78116	0.01557	-0.17547	-0.03113
80.13	-4.03	-0.00344	0.12905	-0.65354	0.01498	-0.16906	-0.02667
80.01	-2.02	0.05440	0.12392	-0.52515	0.01933	-0.15481	-0.04472
80.47	0.01	0.10902	0.12380	-0.37827	0.01492	-0.14408	-0.05958
80.24	2.07	0.18449	0.13091	-0.22353	0.01557	-0.12116	-0.06971
80.24	4.06	0.23497	0.13440	-0.07513	0.01354	-0.12411	-0.07306
80.59	6.00	0.29567	0.14405	0.07547	0.01518	-0.11357	-0.08214
80.59	8.07	0.37050	0.16107	0.23468	0.02397	-0.09341	-0.09937
80.59	10.12	0.46875	0.18743	0.38740	0.02620	-0.08054	-0.10575
80.36	8.03	0.36837	0.16126	0.23029	0.02808	-0.09680	-0.10253
80.36	6.06	0.30573	0.14590	0.08083	0.02183	-0.11177	-0.08062
80.36	4.04	0.23167	0.13507	-0.07821	0.01874	-0.12403	-0.07757
80.36	2.07	0.17290	0.12922	-0.22422	0.01758	-0.12658	-0.07426
80.36	-0.01	0.11007	0.12363	-0.37932	0.01499	-0.14025	-0.06126
80.36	-2.02	0.06265	0.12391	-0.52027	0.00826	-0.16371	-0.03232
80.24	-4.04	-0.00036	0.12582	-0.65298	0.01422	-0.16987	-0.02574
80.13	-6.01	-0.07653	0.13180	-0.77800	0.02377	-0.17329	-0.03103
80.24	-8.01	-0.15650	0.14325	-0.90318	0.02731	-0.17991	-0.03986
80.13	-10.04	-0.24255	0.15827	-1.02001	0.02577	-0.18976	-0.03851

Reference Area = 1.43 ft^2 ; Reference Length = 1.26 ft

Run# 246 Test Section Temperature = 70.9 [F] Density = 0.002256 [slug/ft^3]
Reynolds Number/ft= 0.1568563E+07 Static Pressure= 2041.37 [lb/ft^2]

Dynamic Pressure (psf)	Angle of Attack (deg)	C_L	C_D	C_PM	C_RM	C_YM	C_SF
80.36	2.03	0.22103	0.13189	-0.25372	0.00789	-0.12360	-0.01290
80.13	0.00	0.19290	0.12171	-0.40636	0.00406	-0.13186	-0.00236
80.13	-2.03	0.12499	0.11372	-0.54745	0.00757	-0.14610	0.00053
80.13	-4.03	0.06309	0.11336	-0.67494	0.01219	-0.16053	0.00386
79.90	-6.02	-0.00164	0.11325	-0.79988	0.01565	-0.16207	-0.00055
80.36	-8.07	-0.08124	0.11925	-0.92272	0.02337	-0.16544	-0.00637
80.13	-10.05	-0.16698	0.13160	-1.03640	0.03118	-0.16622	-0.01293
80.13	-8.00	-0.08427	0.12118	-0.92297	0.02445	-0.16576	-0.00882
80.24	-6.00	-0.01554	0.11369	-0.79730	0.02133	-0.16322	-0.00792
80.24	-4.03	0.05272	0.11064	-0.67555	0.01262	-0.16088	0.00035
80.24	-2.00	0.12448	0.11498	-0.54418	0.00552	-0.14904	0.00014
79.90	0.01	0.17908	0.12112	-0.40931	0.00982	-0.13442	-0.00902
80.01	2.03	0.22937	0.13158	-0.25338	0.00766	-0.12289	-0.01181
80.24	4.05	0.27933	0.13973	-0.10170	0.00819	-0.11371	-0.02361
80.24	6.03	0.35286	0.15714	0.04894	0.00856	-0.10850	-0.02925
80.01	8.00	0.42530	0.17858	0.19438	0.00805	-0.10303	-0.03729
80.13	10.00	0.50718	0.20642	0.33547	0.01306	-0.08579	-0.05008

Reference Area = 1.43 ft^2 ; Reference Length = 1.26 ft

Run# 309 Test Section Temperature = 77.9 [F] Density = 0.002205 [slug/ft^3]
Reynolds Number/ft= 0.1552568E+07 Static Pressure= 2023.99 [lb/ft^2]

Dynamic Pressure (psf)	Angle of Attack (deg)	C_L	C_D	C_PM	C_RM	C_YM	C_SF
80.13	2.05	0.13218	0.12300	-0.24880	0.01708	-0.10852	-0.07676
80.01	-0.01	0.09182	0.12054	-0.38668	0.01197	-0.12714	-0.06113
80.01	-2.00	0.05758	0.12236	-0.52235	0.01341	-0.14826	-0.04892
79.90	-4.01	0.01356	0.12329	-0.64277	0.01253	-0.16717	-0.02438
80.13	-6.01	-0.01452	0.12352	-0.76040	0.01419	-0.17323	-0.02509
80.24	-8.02	-0.06198	0.12680	-0.87754	0.02435	-0.17873	-0.03439
80.13	-10.04	-0.13356	0.13611	-0.98750	0.03006	-0.18950	-0.04060

Reference Area = 1.43 ft^2 ; Reference Length = 1.26 ft

REFERENCES

1. Sheehy, Thomas W.; and Clark, David R.: A General Review of Helicopter Rotor Hub Drag Data. 31st Annual National Forum of the American, May 1975.

2. Sheehy, Thomas W.: A Method for Predicting Helicopter Hub Drag. Army Air Mobility Research and Development Laboratory, AD-A021 201, Jan. 1976.

3. Keys, C. N. and Rosenstein, H. J.: Summary of Rotor Hub Drag Data. NASA CR-152080, 1978.

4. Wilson, John C.: Wind Tunnel Tests of Models of Rotor Head Fairing. UCA Research Dept., Report UAR-0495, Aug. 7, 1959.

5. Foster, R. D.: Results of the 1/2 Scale HU-1 and High Speed Helicopter Pylon and Hub Model Wind Tunnel Investigation. Bell Helicopter Company, Report 8025-099-012, March 1961.

6. Smoke Tunnel Test of Faired Rotor Hubs on the 1/8-Scale HC-1B Model. The Boeing Company Vertol Division, Report R-359, Sept. 1963.

7. Results of Rotor Hub Fairing Analytical Study. The Boeing Company Vertol Division, Report R-356, Sept. 1964.

8. Young, Larry A.; and Graham, David R.: Experimental Investigation of Rotorcraft Hub and Shaft Fairing Drag. AIAA 4th Applied Aerodynamics Conference, June 1986.

9. Young, Larry A.; Graham, David R.; Stroub, Robert H.; and Louie, Alexander W.: Reduction of Hub- and Pylon-Fairing Drag. 43rd Annual Forum and Technology Display of the American Helicopter Society, May 1987.

10. Stroub, Robert H.; Young, Larry A.; Graham, David R.; and Louie, Alexander W.: Investigation of Generic Hub Fairing and Pylon Shapes to Reduce Hub Drag. 13th European Rotorcraft Forum, Sept. 1987.

11. Graham, D. R.; Sung, D. Y.; Young, L. A.; Louie, A. W.; and Stroub, R. H.: An Experimental Study of Helicopter Hub Fairing and Pylon Interference Drag. NASA TM-101052, Jan. 1989.

12. Louie, A. W.: Evaluation of VSAERO in Prediction of Aerodynamic Characteristics of Helicopter Hub Fairings. NASA TM-101048, Feb. 1989.

13. Felker, Fort F.: An Experimental Investigation of Hub Drag on the XH-59A. AIAA 3rd Applied Aerodynamics Conference, Oct. 1985.

14. Montana, Peter S.: Experimental Evaluation of Analytically Shaped Helicopter Rotor Hub-Pylon Configurations using the Hub Pylon Evaluation Rig. David W. Taylor Naval Ship Research And Development Center, Report ASED-355, July 1976.

15. Logan, A. H.; Prouty, R. W.; and Clark, D. R.: Wind Tunnel Tests of Large- and Small-scale Rotor Hubs and Pylons. USAAVRADCOM TR 80-D-21, April 1981.

16. Montana, Peter S.: Helicopter Drag Technology Program Fiscal 1973 Progress Report. Naval Ship Research and Development Center, Sept. 1983.

Table I. - TEST MATRIX SHOWING PYLON AND HUB FAIRING COMBINATIONS

C INDICATES CONFIGURATION NUMBER

PYLON	HUB FAIRING												
	H10	H20	H30	H40	H50	H60	H220	H230	H240	H250	H260	H270	H280
S40	C21; •c	C12; •b	C13; •b	C14; •b	C06; •a,b,c,d	C15; •b	C34; •d	C35; •d	C07; •a	C08; •a	C09; •a	C10; •a	C11; •a
S40 (0.25-in. gap)	C22; •c				C28; •c								
S40 (0.50-in. gap)	C23; •c				C29; •c								
S40 (0.75-in. gap)	C24; •c				C30; •c								
S40 (1-in. gap)	C25; •c				C31; •c								
S40 (3-in. gap)	C26; •c				C32; •c								
S80		C16; •b	C17; •b	C18; •b	C19; •b	C20; •b							
S40 (6 in. high)					C36; •e								
S40 (4 in. high)					C37; •e								
S40 (2 in. high)					C38; •e								
S40 + W1 (1-in. gap)	C40; •f				C42; •f								
S40 + W2 (1-in. gap)	C41; •f				C43; •f								
S40 + W1	C44; •f				C46; •f								
S40 + W2	C45; •f				C47; •f								

Notes:

- •W- wake shield
- •a- hub fairing diameter sweep (constant thickness)
- •b- hub fairing camber sweep (constant diameter and thickness)
- •c- hub/pylon gap width (constant height between hub fairing and fuselage)
- •d- hub fairing thickness sweep (constant diameter)
- •e- pylon height sweep
- •f- wake shield sweep

Figure 1. – Model installation in the NASA Langley 14- by 22-Foot Wind Tunnel.

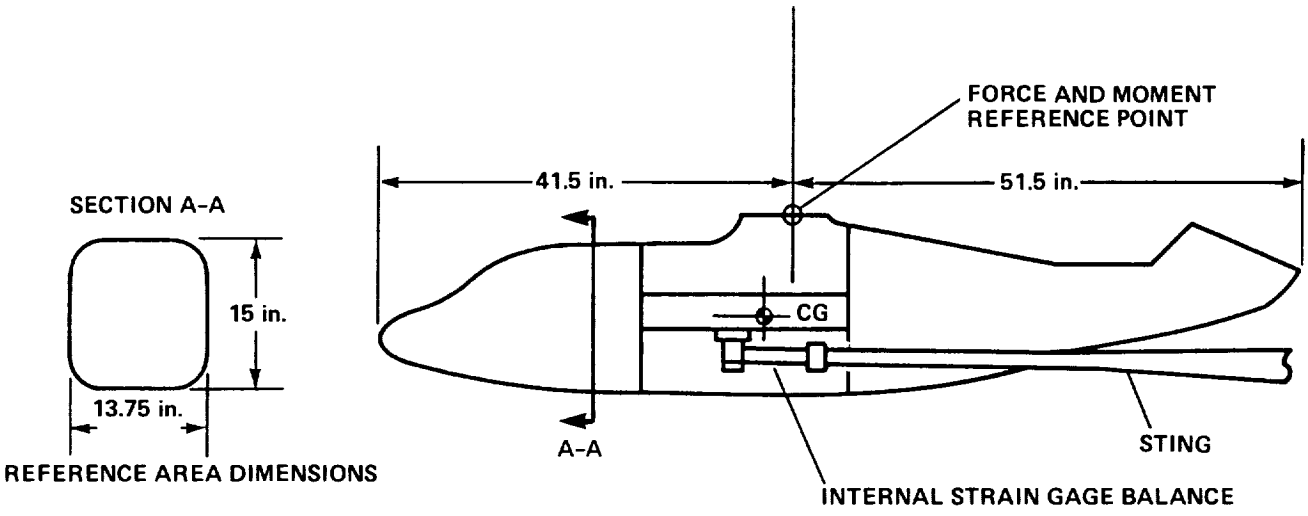

Figure 2. – Model dimensions and mounting scheme.

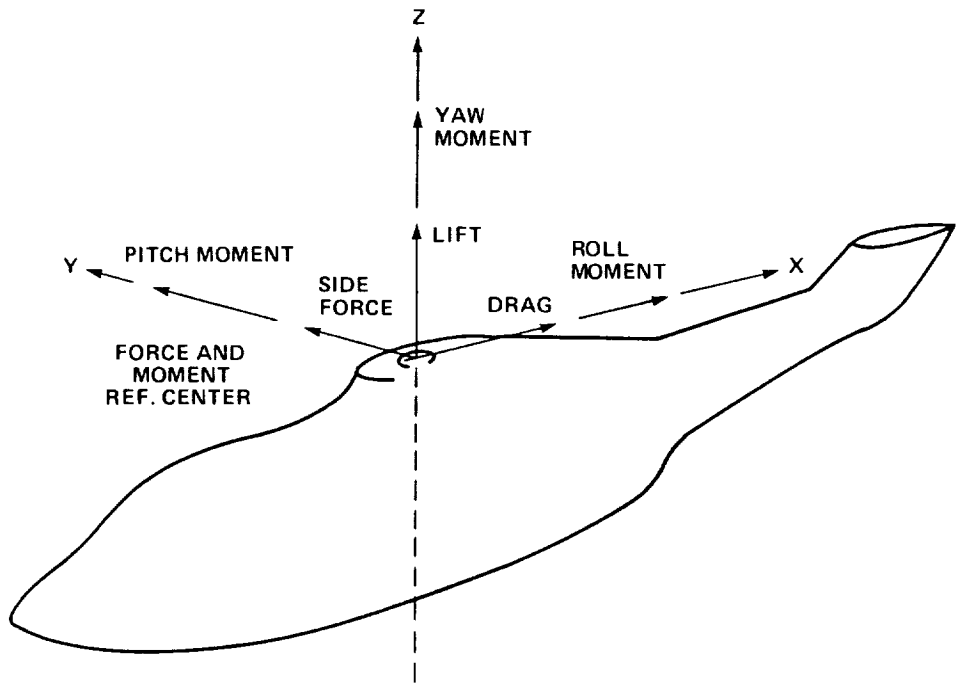

Figure 3. – Reference coordinate system.

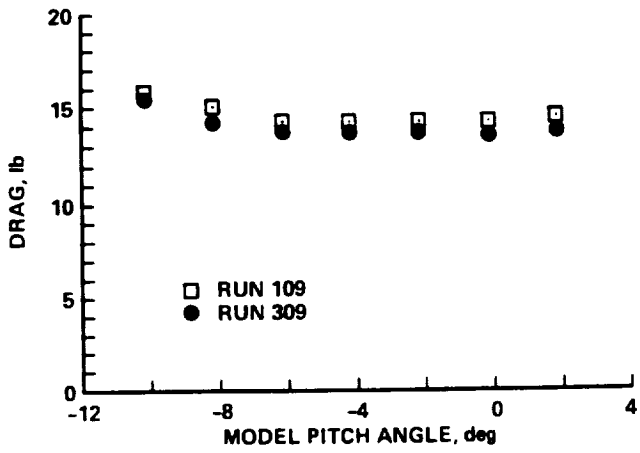

Figure 4. – Data repeatability, H50-S40 configuration.

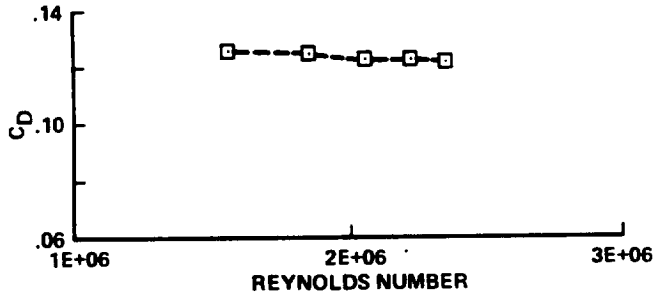

Figure 5. – Reynolds number effects.

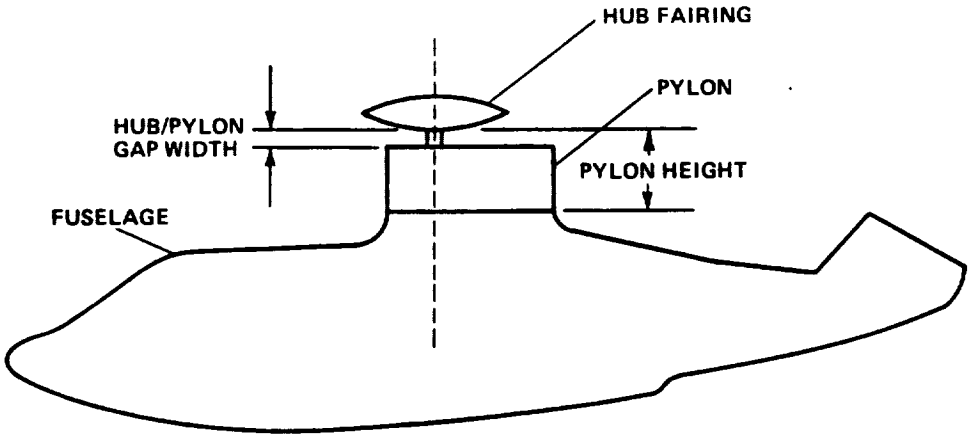

Figure 6. – Test configuration.

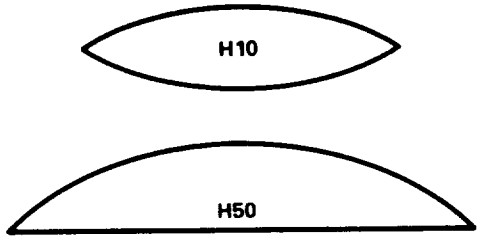

	H10	H50
DIAMETER, ft	0.92	1.25
THICKNESS RATIO (FRACTION OF DIAMETER)	0.24	0.18
CAMBER (FRACTION OF DIAMETER)	0.00	0.09
LOWER SURFACE SECOND DERIVATIVE AT CENTER	-0.45	0.00
UPPER SURFACE SECOND DERIVATIVE AT CENTER	0.45	-0.62

Figure 7. – Hub fairing cross sections: H10 and H50 hub fairing.

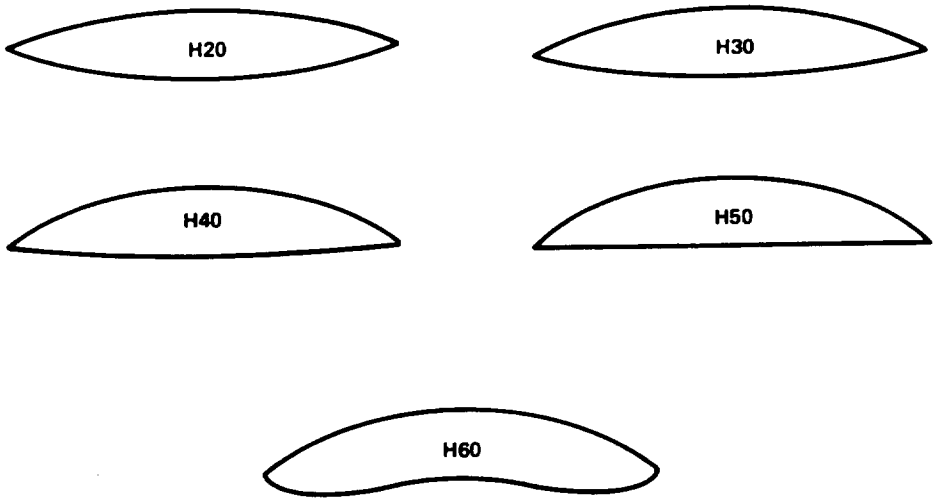

	H20	H30	H40	H50	H60
DIAMETER, ft	1.25	1.25	1.25	1.25	1.25
THICKNESS RATIO (FRACTION OF DIAMETER)	0.18	0.18	0.18	0.18	0.18
CAMBER (FRACTION OF DIAMETER)	0.00	0.03	0.06	0.09	0.11
UPPER SURFACE SECOND DERIVATIVE AT CENTER	-0.34	-0.44	-0.54	-0.62	-0.60
LOWER SURFACE SECOND DERIVATIVE AT CENTER	0.34	0.23	0.12	0.00	-1.00

Figure 8. – Hub fairing cross sections: variation of camber.

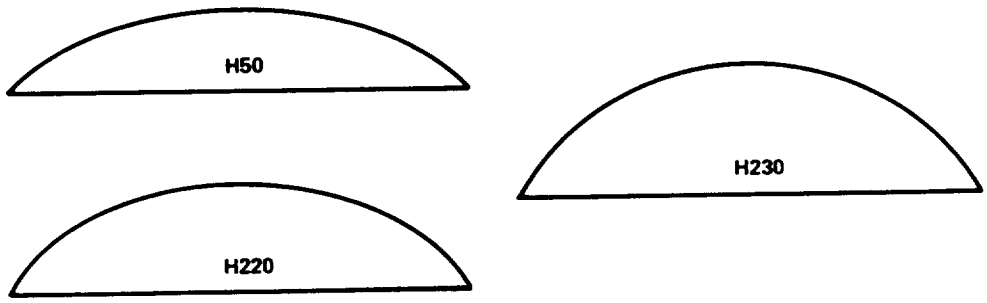

	H50	H220	H230
DIAMETER, ft	1.25	1.25	1.25
THICKNESS RATIO (FRACTION OF DIAMETER)	0.18	0.24	0.29
CAMBER (FRACTION OF DIAMETER)	0.09	0.12	0.14
UPPER SURFACE SECOND DERIVATIVE AT CENTER	-0.62	-0.78	-0.87

Figure 9. – Hub fairing cross sections: variation of thickness ratio (constant diameter).

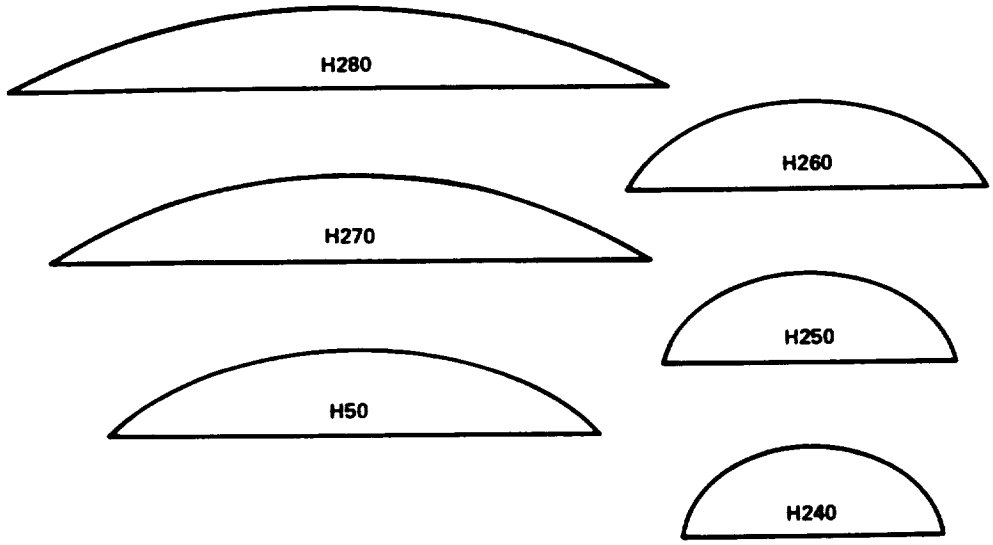

	H260	H270	H50	H260	H250	H240
DIAMETER, ft	1.67	1.46	1.25	0.92	0.74	0.66
THICKNESS RATIO (FRACTION OF DIAMETER)	0.13	0.15	0.18	0.24	0.29	0.33
CAMBER (FRACTION OF DIAMETER)	0.07	0.08	0.09	0.12	0.15	0.17
UPPER SURFACE SECOND DERIVATIVE AT CENTER	-0.49	-0.55	-0.62	-0.78	-0.87	-0.92

Figure 10. – Hub fairing cross sections: variations of thickness ratio (constant thickness).

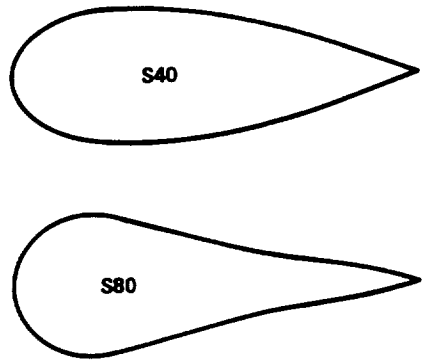

	S40	S80
CHORD LENGTH, ft	1.58	1.58
LOCATION OF MAXIMUM THICKNESS (FRACTION OF CHORD LENGTH)	0.30	0.20
TRAILING EDGE SLOPE	-1.17	-1.17
THICKNESS RATIO	0.34	0.34

Figure 11. – Shaft fairing cross sections: S40 and S80 pylons.

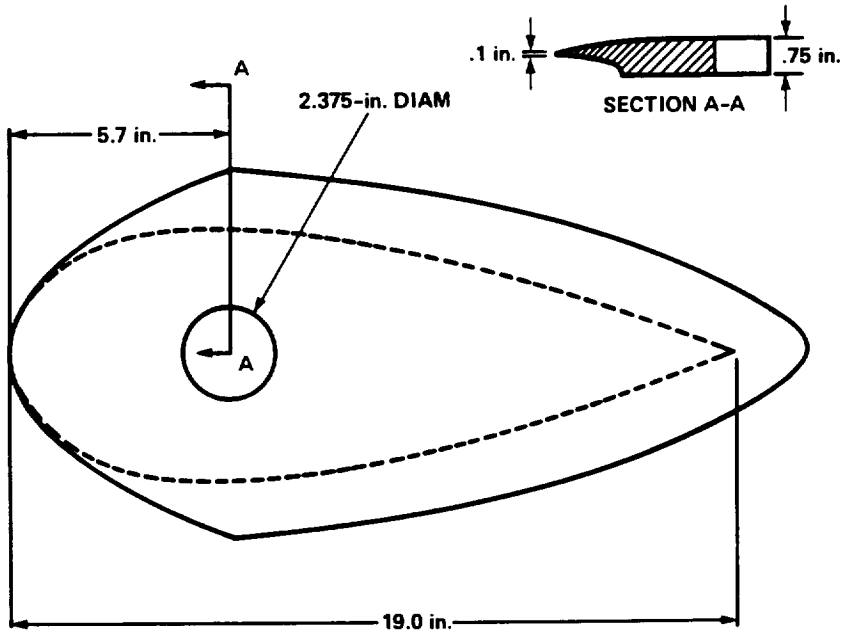

a) W1 WAKE SHIELD

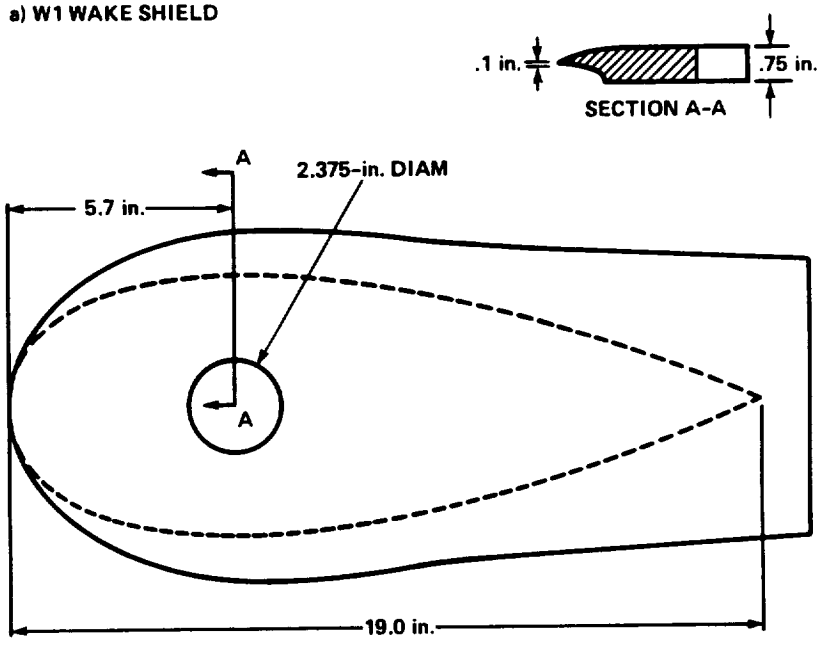

b) W2 WAKE SHIELD

Figure 12. – Top views of the wake shields tested.

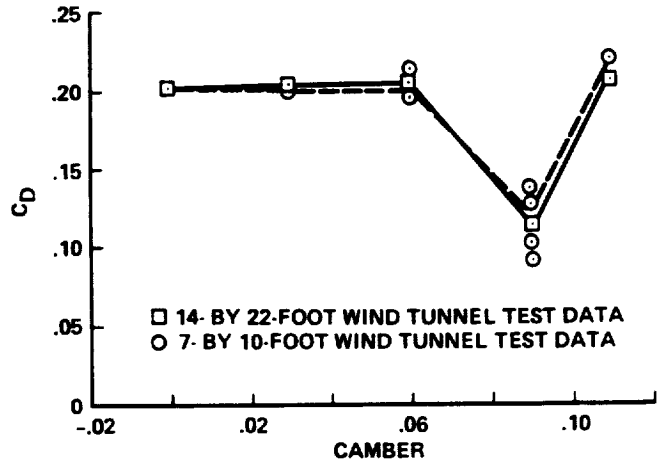

Figure 13. – 14- by 22-Foot and 7- by 10-Foot Wind Tunnel test data comparison, effect of hub fairing camber on drag with S80 pylon.

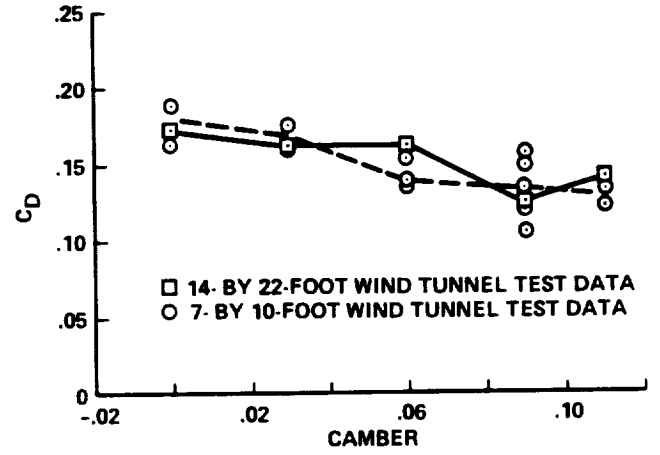

Figure 14. – 14- by 22-Foot and 7- by 10-Foot Wind Tunnel test data comparison, effect of hub fairing camber on drag with S40 pylon.

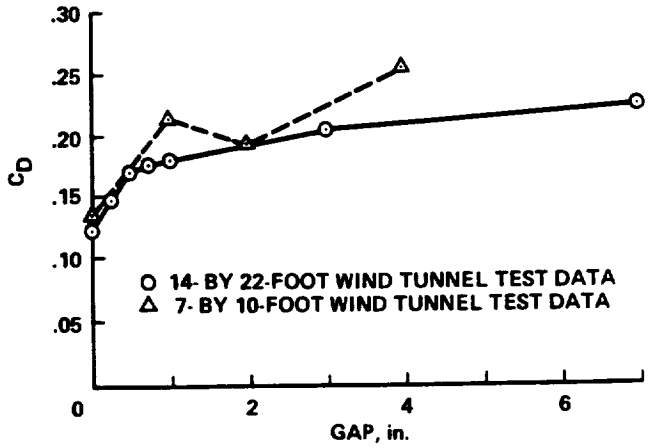

Figure 15. – 14- by 22-Foot and 7- by 10-Foot Wind Tunnel test data comparison, hub/pylon fairing gap effect on drag with H50 hub fairing, S40 pylon.

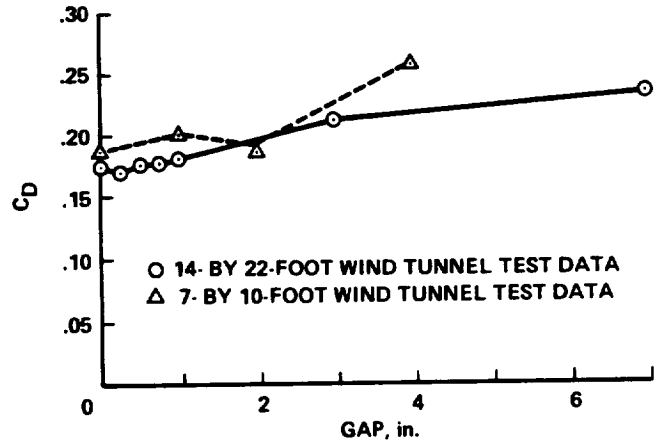

Figure 16. – 14- by 22-Foot and 7- by 10-Foot Wind Tunnel test data comparison, hub/pylon fairing gap effect on drag with H10 hub fairing, S40 pylon.

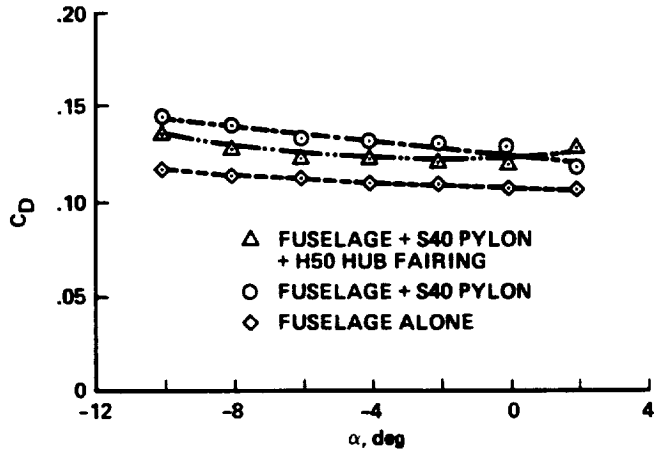

Figure 17. – Interference effects between hub fairing and pylon.

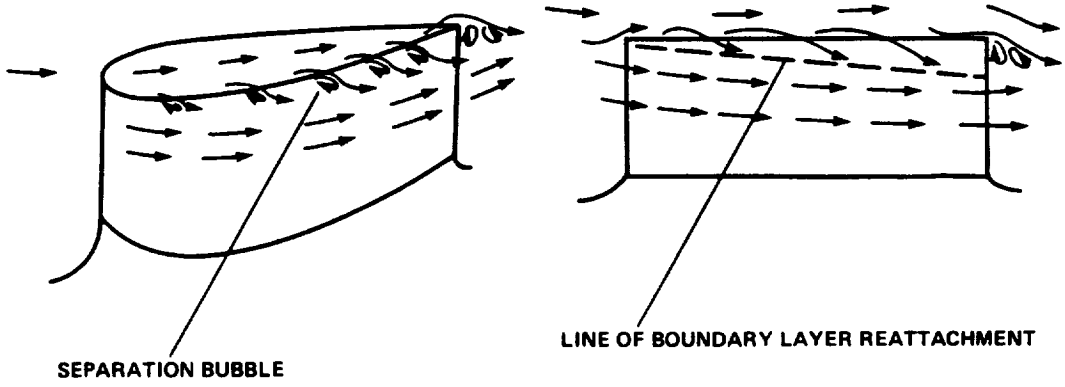

Figure 18. – Flow over S40 pylon without hub fairing at a negative angle of attack.

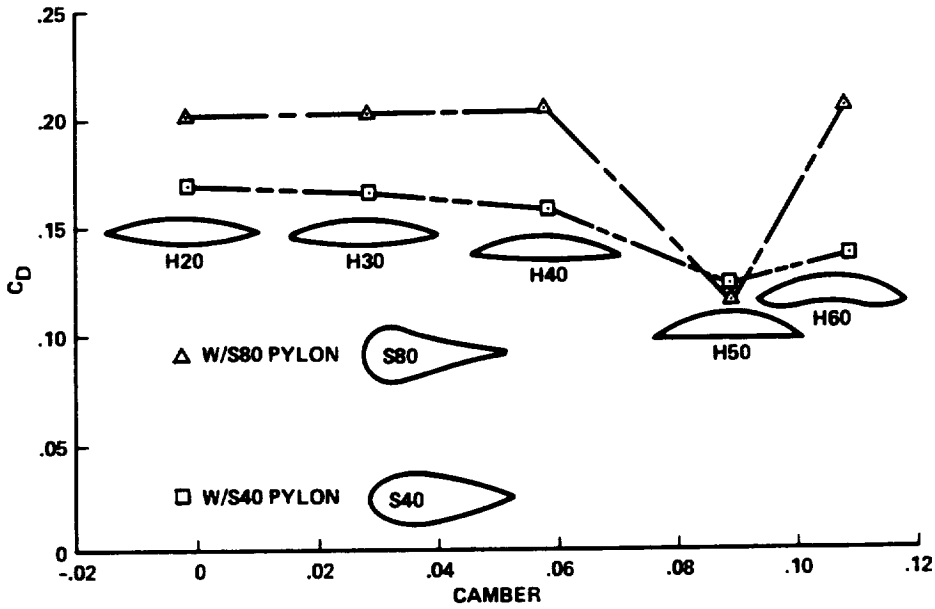

Figure 19. – Effect of hub fairing camber on drag.

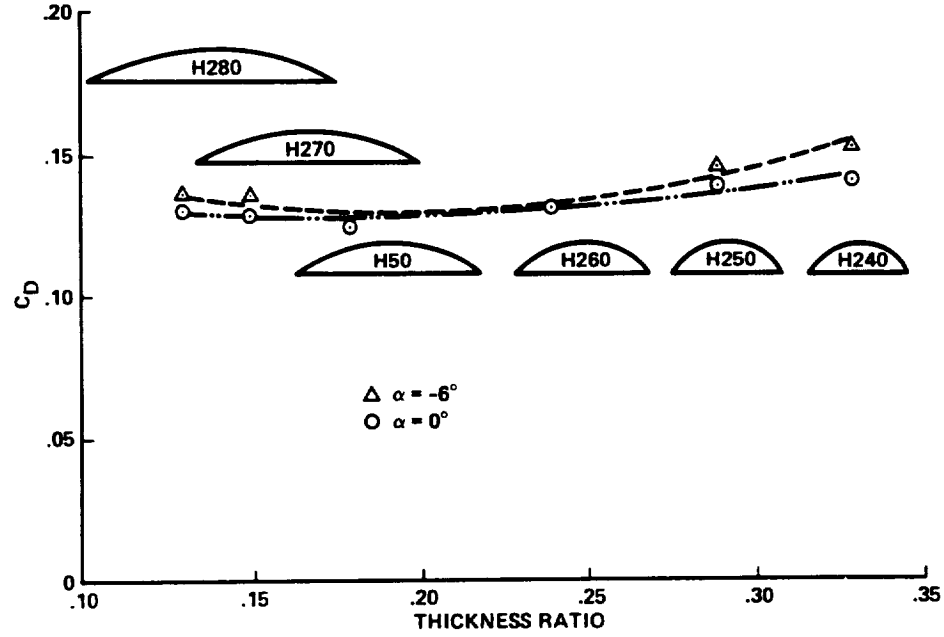

Figure 20. – Drag as a function of hub fairing thickness ratio (constant thickness).

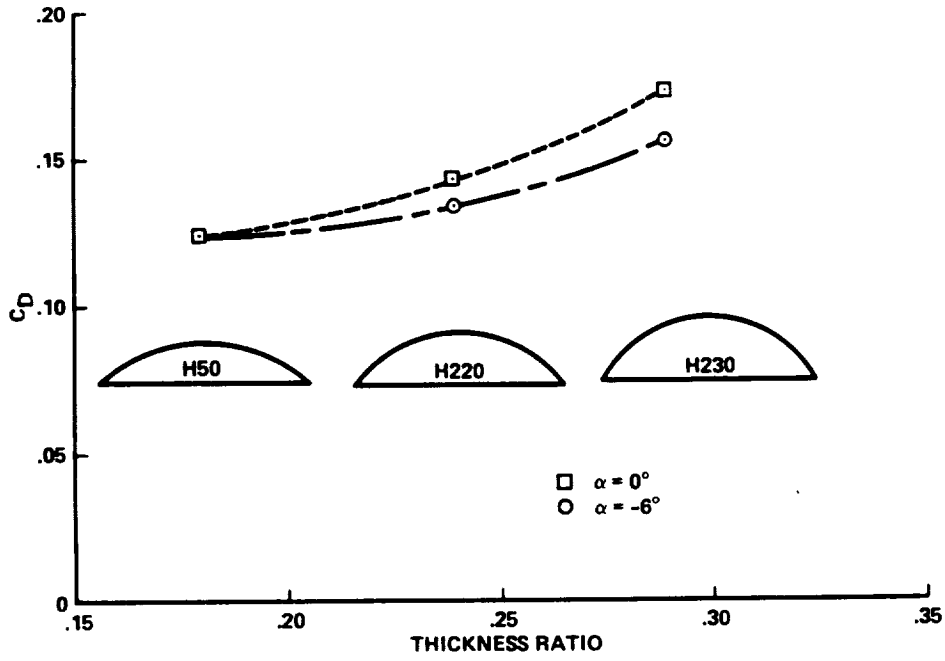

Figure 21. – Drag as a function of hub fairing thickness ratio (constant diameter).

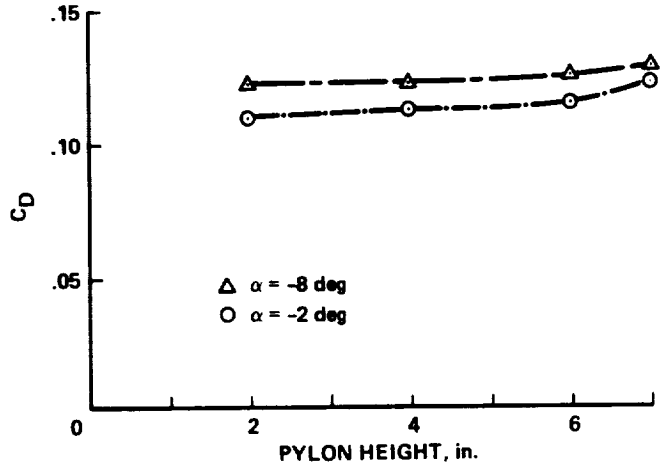

Figure 22. – Effect of pylon height on drag.

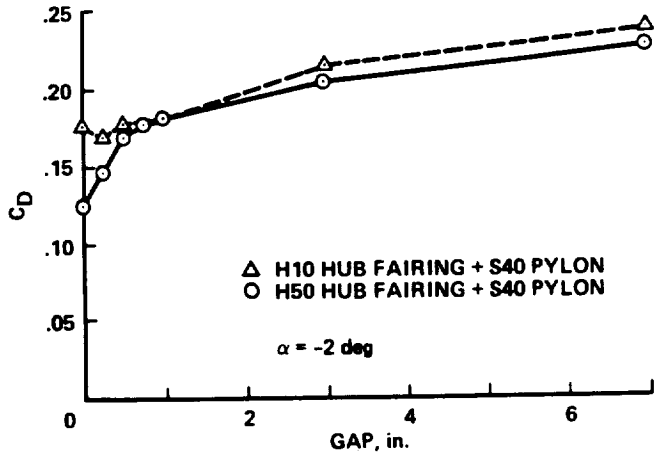

Figure 23. – Effect of hub/pylon gap width on drag (cambered H50 and symmetrical H10 hub fairings with S40 pylon).

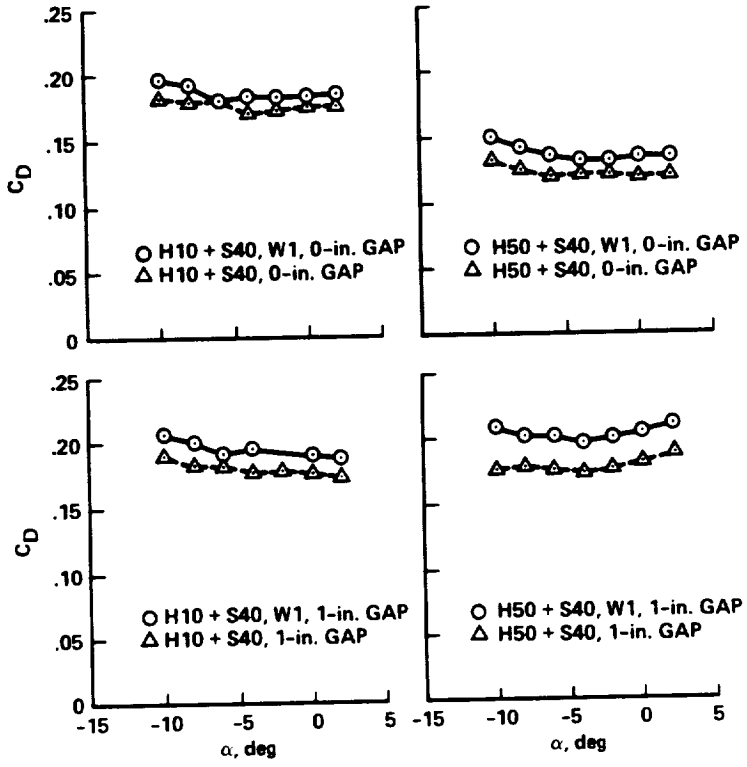

Figure 24. – Effect of pylon wake shield (W1) on drag.

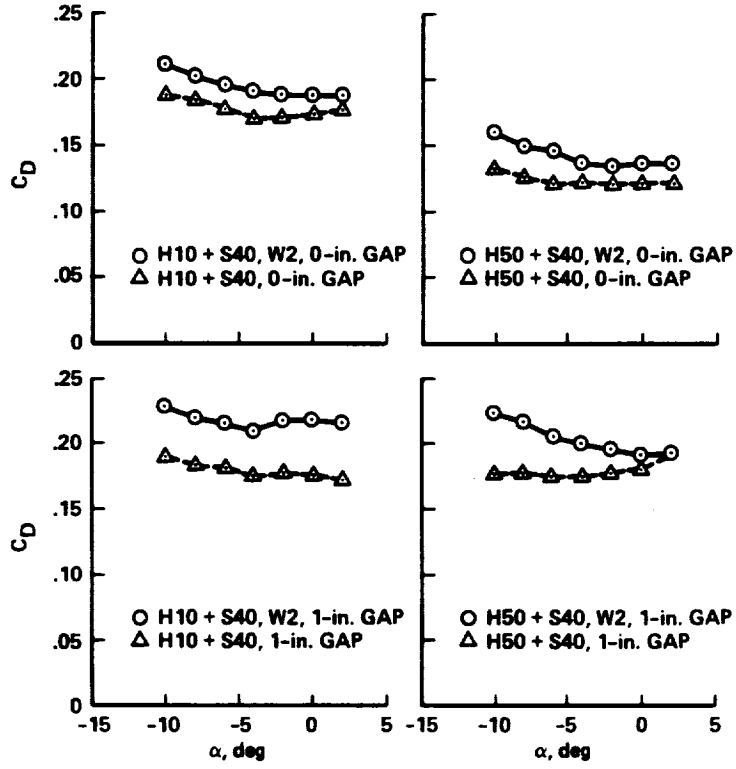

Figure 25. – Effect of pylon wake shield (W2) on drag.

NASA
National Aeronautics and Space Administration

Report Documentation Page

1. Report No.	2. Government Accession No.	3. Recipient's Catalog No.
NASA TM-102182		

4. Title and Subtitle
An Experimental Investigation of Helicopter Rotor Hub Fairing Drag Characteristics

5. Report Date
September 1989

6. Performing Organization Code

7. Author(s)
D. Y. Sung (Sterling Software Corp., Palo Alto, CA), M. B. Lance (Planning Research Corp., Hampton, VA), L. A. Young, and R. H. Stroub

8. Performing Organization Report No.
A-89096

10. Work Unit No.
505-61-51

9. Performing Organization Name and Address
Ames Research Center
Moffett Field, CA 94035

11. Contract or Grant No.

13. Type of Report and Period Covered
Technical Memorandum

12. Sponsoring Agency Name and Address
National Aeronautics and Space Administration
Washington, DC 20546-0001

14. Sponsoring Agency Code

15. Supplementary Notes
Point of Contact: L. A. Young, Ames Research Center, MS T-42, Moffett Field, CA 94035
(415) 694-4022 or FTS 464-4022

16. Abstract

A study was done in the NASA 14- by 22-Foot Wind Tunnel at Langley Research Center on the parasite drag of different helicopter rotor hub fairings and pylons. Parametric studies of hub-fairing camber and diameter were conducted. The effect of hub fairing/pylon clearance on hub fairing/pylon mutual interference drag was examined in detail. Force and moment data are presented in tabular and graphical forms. The results indicate that hub fairings with a circular-arc upper surface and a flat lower surface yield maximum hub drag reduction; and clearance between the hub fairing and pylon induces high mutual-interference drag and diminishes the drag-reduction benefit obtained using a hub fairing with a flat lower surface. Test data show that symmetrical hub fairings with circular-arc surfaces generate 74% more interference drag than do cambered hub fairings with flat lower surfaces, at moderate negative angle of attack.

17. Key Words (Suggested by Author(s))	18. Distribution Statement
Interference drag Rotor hub fairings Aerodynamic interactions	Unclassified-Unlimited Subject Category - 02

19. Security Classif. (of this report)	20. Security Classif. (of this page)	21. No. of Pages	22. Price
Unclassified	Unclassified	60	A04

For sale by the National Technical Information Service, Springfield, Virginia 22161